Δ degrees of freedom in trinuclei: I. The Hannover one-Δ model

A. Picklesimer,[1] R. A. Rice,[1,2] and R. Brandenburg[1,3]
[1]*Physics Division, Los Alamos National Laboratory, Los Alamos, New Mexico 87545*
[2]*Department of Physics, Purdue University, West Lafayette, Indiana 47907*
[3]*Institute for Physics, University of Basel, 3056 Basel, Switzerland*
(Received 8 April 1991)

The shift in binding energy that results from allowing one explicit Δ in the triton is studied using the Hannover one-Δ force model. The one-Δ analysis extends through $J \leq 4$, subject only to $L(N\Delta) \leq 4$. Our main result is a 103-channel triton binding energy of 7.83 MeV, which corresponds to a net attractive one-Δ effect of 370 keV. The corresponding (repulsive) dispersive effect is found to be 600 keV, so that the full one-Δ three-body-force effect is 970 keV. Appropriately restricted $J \leq 2$ calculations substantiate the basic results of the original Hannover triton calculations, although differences are found. The original $J \leq 2$ figures are in good agreement with our full results and dissecting our results shows this to be largely due to cancellations among the various truncations employed in the original calculations. A numerical correction is obtained for each truncation and these are found to be relatively independent of each other. This forms a reliable basis for subsequent ΔΔ studies. The Hannover one-Δ model is also critically examined for physical consistency and the $^1S_0$ effective range is found to be about 0.1 fm too low, a defect which could be responsible for about half of the net 370-keV increase in triton binding. The approach, methods, and numerical checks that underlie our investigations are also detailed.

I. INTRODUCTION

The classical picture of the nucleus is that it is a composite structure with protons and neutrons (nucleons) as its constituent particles. Also basic to most nuclear calculations is the assumption of the validity of a description of the nucleus via the nonrelativistic Schrödinger equation. Calculations of nuclear properties then proceed on the assumption that the nucleons interact via an instantaneous nucleon-nucleon (*NN*) potential.

The success of nuclear physics in understanding many of the properties of nuclei—from the semiempirical mass formula, through the shell model and rotational model predictions of energy spectra—indicates that the picture outlined in the preceding paragraph is a sensible one. It is certainly, however, an oversimplified picture. The nucleons themselves are known to be composite particles, with resonant states to which they can be excited. The *NN* interaction, at least its longest-range component, is thought to be mediated via the exchange of virtual mesons. That the presence of the virtual mesons can significantly affect the electromagnetic properties of nuclei is well established [1]. A dynamical description based on nucleons interacting via meson exchange also implies nontrivial relativistic corrections. It is of interest then to ask the following: At what level does the "simple" picture of the nucleus start to deviate substantially from reality? To what extent and at what level must subnucleonic degrees of freedom be incorporated into the model of the nucleus in order to accurately predict nuclear properties? What picture of nuclear dynamics best corresponds to actual physical reality?

The solution of the many-body Schrödinger equation is a formidable task; so much so that only the simplest of nuclear systems are amenable to direct calculation. This impedes investigations of the above questions, since deficiencies in the model are, or could be, masked by the approximations used to solve the numerical problem. Here is where the three-body problem is of paramount interest. The numerical difficulties of solving the three-body Faddeev equations [2,3] have been overcome [4]. By this it is meant that, given a system of three nucleons and the potential through which they interact, the solution of the Schrödinger equation can be found to desired accuracy. Differences between predictions of the model and the physical data must then be ascribed either to a poor choice for the *NN* potential or to oversimplification in the standard view of the nucleus. When one goes beyond a purely phenomenological description of the *NN* potential and attempts to describe the *NN* interaction from a more fundamental viewpoint, these two possibilities become entwined.

Computationally, the simplest of all three-nucleon properties is the binding energy of the triton, $E_T = 8.48$ MeV. It is thus remarkable that calculations using the best available "realistic" potentials consistently fail to reproduce this number, by 0.5–1.0 MeV. A "realistic" potential is one which fits well the deuteron properties and the *NN* scattering data from threshold up to $E_{\rm lab} = 350$ MeV. Examples of "realistic" potentials which have been used are the Reid [5], Paris [6], V14 [7], and Bonn [8,9] potentials. If one relaxes somewhat this definition of "realistic," then the Bonn momentum space one-boson-exchange potential (OBEPQ) potential [10], which begins to deviate from the *NN* scattering data above ~100 MeV, but predicts a triton binding energy of 8.35 MeV [11], should also be included. (See, however, Ref. [12].) The salient fact is that one is unable to simul-

taneously reproduce the *NN* data and predict the triton binding energy. This is a clear signal of an inadequacy of the simple picture of nuclei.

The triton binding-energy defect could be accounted for by introduction of a three-nucleon potential into the three-body Hamiltonian. This approach has the advantage that the simple picture of the nucleus as a composite of nucleons can be maintained. It is only necessary to modify the interaction Hamiltonian. The existence of a three-nucleon (*NNN*) force is, nonetheless, a direct consequence of the underlying compositeness of the nucleon, as well as the exchange mechanism thought to be responsible for the interaction between nucleons. A typical *NNN* force is depicted in Fig. 1, in the context of time-ordered perturbation theory (TOPT). This type of diagram, with the exchanged particle taken to be a pion, figures in the calculation of every *NNN* potential [13–15]. The corresponding potential mediated through the exchange of heavier mesons is of shorter range and is assumed to be of less import. Triton binding calculations [16–21] using this type of *NNN* potential in combination with one of the "realistic" *NN* potentials above show that it is always possible to explain the discrepancy between the experimental and numerical results on this basis. Unfortunately, the size of the contribution from these *NNN* potentials is strongly dependent on the cutoff parameter of the pion-nucleon form factor, and varying this parameter allows one to obtain greatly varying results, including the correct binding energy for most combinations of two- and three-body potentials. This adds a strongly phenomenological component to the three-body system itself and detracts from the status of the triton as a dynamical proving ground.

Ideally, one would explicitly treat the degrees of freedom which are ignored in the "nucleons-only" approach. While this is beyond our present capabilities, some attempts in this direction have been made. These consist of coupled-channel models which treat one of the nucleon resonances, the Δ isobar, as a stable particle, which, through a potential interaction, can make transitions to and from the nucleon (intrinsic) state. There exist today several potential models with this added degree of freedom [7,22–24]. Figure 2 schematically depicts such potential models. These potentials, which are fitted to the *NN* data, have so far not been used in trinuclear calculations. Use of these potentials in a coupled-channel approach to the triton, in which the nucleon and the Δ are treated on an equal footing, includes naturally three-body forces typified by the diagrams of Fig. 3. One disadvantage of this method is that it ignores all but the Δ contribution to the three-body force. Another is that it does not allow the inclusion of all types of meson-theoretic Δ diagrams of a given order on an equal basis. Only those Δ diagrams which can be expressed in terms of baryons-

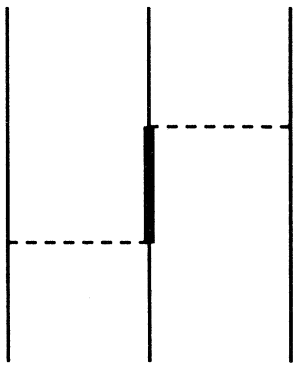

FIG. 1. The standard example of a three-nucleon force diagram. The thin lines denote nucleons, the thick lines denote a nucleon resonance, and dashed lines denote exchanged mesons.

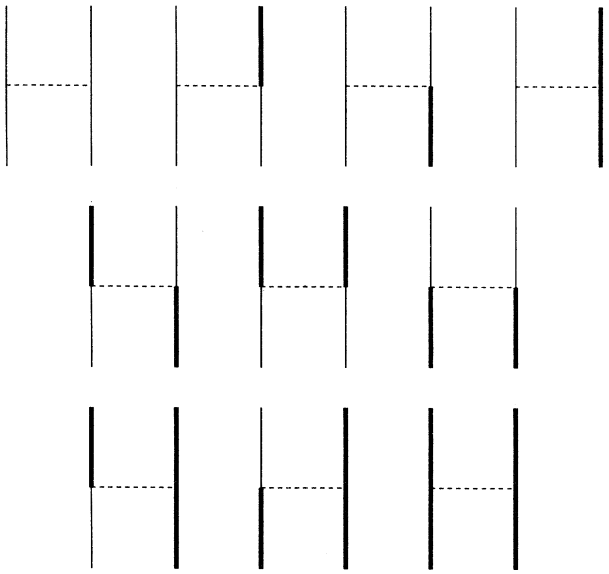

FIG. 2. The diagrams which schematically represent the two-body potentials of the coupled-channel approach. The Hannover single-Δ model has only components of the first three types.

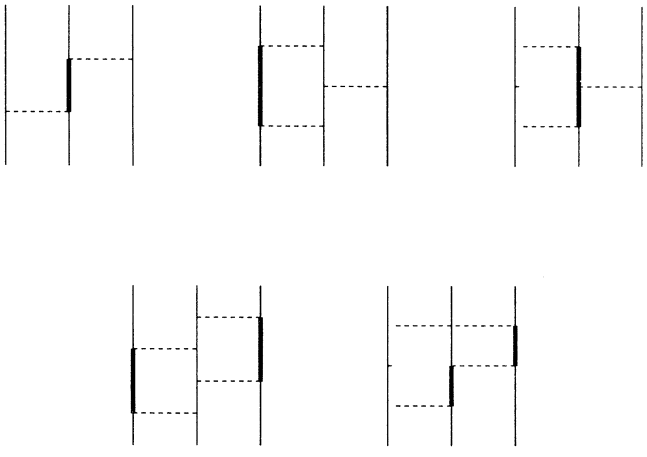

FIG. 3. Examples of three-body forces included in triton calculations based on the coupled-channel approach. The Hannover one-Δ model includes only the first two examples.

only states (NN, $N\Delta$, NNN, $NN\Delta$, $N\Delta\Delta$, etc.) and transitions between them fit naturally into the coupled-channel scheme at each order. Two- and three-body diagrams in which a transition to a new intrinsic baryon state occurs, but in which this new state is always accompanied by mesons in flight, are not included explicitly by the coupled-channel approach. For example, Fig. 4 shows some typical two- and three-body diagrams (in TOPT) which do not fit into the coupled-channel scheme. The two-body diagrams of Fig. 4(a) are, at best, included in the two- and three-body systems only implicitly through parameter fits to the two-body data. Three-body diagrams of the type depicted in Fig. 4(b) are entirely omitted in the coupled-channel scheme. The advantages of the coupled-channel approach are, firstly, that it is not restricted to only the long-range π-exchange contribution, but has also the short-range ρ-exchange contribution to the three-body force if this is explicitly included in the potential model. Secondly, those NN and NNN forces which are included are treated in a unified and consistent manner. Such consistency is of obvious importance.

These ideas have been implemented in the pioneering work of the Hannover group [25–27], who calculated triton properties with Δ degrees of freedom, although in a model restricted to allowing only one Δ in the three-body system. Due to this restriction, the Hannover group chose not to use any of the available NN potentials which include the Δ-isobar excitation, but rather to construct an NN-$N\Delta$ potential and to modify the Paris [6] potential accordingly for use as their NN-NN interaction. One of the more important results of the Hannover calculations was showing the significance of what they named the "dispersive effects" of the diagram in Fig. 5. The calculations mentioned previously, which modify the three-body interaction Hamiltonian through the addition of a three-body force, have shown that the contribution to the triton binding energy from diagrams of the type depicted in Fig. 1 is appreciable. The Hannover calculation showed, in addition, that the contribution from the corresponding dispersive diagram (Fig. 5) is repulsive and about two-thirds the size of the three-body-force contribution of Fig. 1, so that the two largely cancel. These dispersive diagrams are an integral part of the NN interaction. It is presumed in calculations which simply add together a two- and three-body interaction that these diagrams are sufficiently well represented in the NN interaction simply through the process of fitting the NN data using a static potential. To exactly what extent this is a valid assumption has not been fully tested by the Hannover results due to their method of choosing the NN-NN potential. However, it is evident that the question of the dispersive effect can never be adequately addressed by static potential models. This too raises serious questions about the applicability of the "nucleons-only" approach to the description of the triton. This circumstance also underscores an advantage of the coupled-channel approach, namely, that particular dispersive diagrams and their three-body-force analogs are either consistently included or neglected.

This work is the first in a series of papers which will implement the inclusion of Δ degrees of freedom in coupled-channel calculations of the triton binding energy and other physical properties. This first paper is restricted to single-Δ excitation using the Hannover potential model; this restriction is largely a tactical one and subsequent papers will report results from ΔΔ and ΔΔΔ studies which incorporate more sophisticated $N\Delta$ and ΔΔ interactions. The technical apparatus needed for these extensions of the present investigations is already in hand and a few calculations allowing both Δ and ΔΔ excitation, and using both the extended Hannover and Argonne V-28 potential models, have, in fact, already been performed. However, once the excitation of more than one Δ at a time is permitted, the number of two- and three-body channels proliferates very rapidly with increasing angular momentum cutoff. For this reason, systematic investigations of the full multiple-Δ problem are best done by building on a careful analysis of the single-Δ case. Because the previous work on single-Δ excitation has been done using the Hannover potential model, it is advantageous to begin here with this model as well. During the process of building up to an analysis which includes the full complexities of multiple-Δ excitation and sophisticated force models, it is most efficient to focus on one representative quantity, so that our initial investiga-

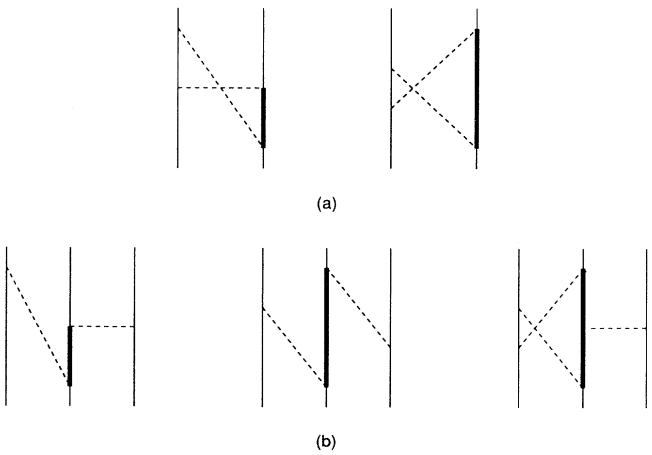

FIG. 4. Typical (a) two-body and (b) three-body Δ diagrams of TOPT which do not fit into the coupled-channel scheme.

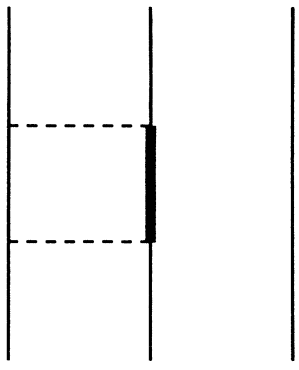

FIG. 5. The stereotypical three-body dispersive diagram.

tions are concentrated mainly on the triton binding energy, E_T.

Thus, this paper is restricted to single-Δ excitation and concentrates for the most part on predictions for the triton binding energy. The main goals of this paper are (1) to obtain an unambiguous result for the one-Δ contribution to the triton binding using the Hannover force model; (2) to substantiate the results obtained previously by the Hannover group, given the limitations of their channel-truncation scheme; (3) to gauge the accuracy and reliability of the Hannover channel-truncation scheme and find the necessary corrections to it, their interplay, and correction methods which can be applied by hand; (4) to lay the groundwork for subsequent extensions to multiple-Δ excitation and more sophisticated force models by establishing a reliable channel-truncation and correction scheme from which to begin; and (5) to critically examine the physical consistency of the two- and three-body predictions of the Hannover one-Δ models.

In the next section, the required extensions of the usual three-body Faddeev equation formalism are developed. This provides a concise overview both of the necessary modifications to the usual Faddeev equations and of our methods of treating the generalization to include Δ degrees of freedom, which differ somewhat from previous developments. Section III outlines the Hannover force model, Sec. IV presents our results, and a brief summary follows in Sec. V. A number of ancillary aspects of the development are relegated to appendices. Appendix A gives an expression for the geometrical coefficient, applicable to the case where any number of Δ's may be present, in the form in which we have used it. Appendix B describes the simple technique needed to deal exactly with the $N\Delta$ mass difference in the coupled two- and three-body equations. Appendix C contains a brief discussion of our numerical methods, accuracy and other checks, and an important error-avoidance attribute of our specific computational scheme.

II. FORMALISM

This section defines the basis states which are used in this work and presents the final form of the Faddeev equations which are ultimately solved to obtain the binding energy. Although the Faddeev equations have been presented many times [4], the inclusion of the Δ degrees of freedom adds enough novel features and notational complications that it is worthwhile to give the explicit forms of the equations.

Fundamental to the approach used in this work and to the earlier Hannover calculations [25] is the treatment of the Δ and the nucleon on an equal basis. Indeed, the two particles are treated as identical fermions in the sense of the generalized Pauli principle. To accomplish this, a "nucleonic-spin" (n-spin) quantum number, $n=\frac{1}{2}$, and its z component n_z are introduced. The definition used here is

$$n_z=\begin{cases}-\frac{1}{2}, & \text{nucleon,}\\ +\frac{1}{2}, & \text{delta}\end{cases} . \tag{1}$$

Thus, a general state describing a free particle of momentum $\mathbf{k}$ is

$$|\mathbf{k};s(n_z),s_z;t(n_z),t_z;\tfrac{1}{2},n_z\rangle . \tag{2}$$

The spin and isospin both depend on the n_z quantum number, with the spin given by

$$s(n_z)=\begin{cases}\frac{1}{2}, & n_z=-\frac{1}{2},\\ \frac{3}{2}, & n_z=+\frac{1}{2}\end{cases} . \tag{3}$$

A similar equation holds for the isospin. The mass dependence of the states is not explicitly shown, but is given by

$$m(n_z)=\begin{cases}M_N, & n_z=-\frac{1}{2},\\ M_\Delta, & n_z=+\frac{1}{2}\end{cases} . \tag{4}$$

The two- and three-body basis states are built from products of these vectors.

The general two-body state of good total spin, isospin, and n spin which describes particles (2,3) is

$$|\mathbf{k}_2,\mathbf{k}_3;SS_z;TT_z;NN_z\rangle_1 \tag{5}$$

or

$$|\mathbf{p},\mathbf{P};SS_z;TT_z;NN_z\rangle_1 , \tag{6}$$

where $\mathbf{p}$ and $\mathbf{P}$ are the relative and center-of-mass momenta of the pair, respectively. The subscript on the ket is introduced here in anticipation of the "odd-man-out" notation which will be used for the three-body basis states in which the spectator, or noninteracting particle, is used to label the two-body potentials and states. The spin, isospin, and n-spin state is given by

$$|SS_z;TT_z;NN_z\rangle_1=\sum_{n_{2z},n_{3z}}\langle\tfrac{1}{2}\tfrac{1}{2}n_{2z}n_{3z}|NN_z\rangle|\tfrac{1}{2}n_{2z}\rangle|\tfrac{1}{2}n_{3z}\rangle|[s(n_{2z})s(n_{3z})]SS_z\rangle|[t(n_{2z})t(n_{3z})]TT_z\rangle . \tag{7}$$

Here, as in what follows, the explicit dependence of the states on the spin, isospin, and n spin of the individual particles will be omitted whenever this causes no confusion. The quantity $\langle\frac{1}{2}\frac{1}{2}n_{2z}n_{3z}|NN_z\rangle$ is the standard Clebsch-Gordan coefficient and the spin and isospin kets are just the usual ones.

These states are eigenstates of the free two-body Hamiltonian, h_0,

$$h_0|\mathbf{p},\mathbf{P};SS_z;TT_z;NN_z\rangle=\left[M(N_z)c^2+\frac{\hbar^2p^2}{2\mu(N_z)}+\frac{\hbar^2P^2}{2M(N_z)}\right]|\mathbf{p},\mathbf{P};SS_z;TT_z;NN_z\rangle , \tag{8}$$

where $M(N_z)$ is the mass of the pair

$$M(N_z)=m(n_{2z})+m(n_{3z}) = \begin{cases} 2M_N, & N_z=-1, \\ M_N+M_\Delta, & N_z=0, \\ 2M_\Delta, & N_z=+1, \end{cases} \tag{9}$$

and $\mu(N_z)$ is the reduced mass of the pair. Further, if the partial-wave projection of the two-body state of relative motion is written as

$$|pLM_L;SS_z;TT_z;NN_z\rangle_1 , \tag{10}$$

then, with $E_1=E_{23}$ being the exchange operator for particles 2 and 3,

$$E_1|pLM_L;SS_z;TT_z;NN_z\rangle_1 = (-1)^{(L+S+T+N+1)}|pLM_L;SS_z;TT_z;NN_z\rangle_1 , \tag{11}$$

which expresses the particle-exchange symmetry of the state.

The three-body basis states are now built from the one- and two-body states in a manner completely analogous to that for the more familiar case where only nucleons are allowed in the triton. All calculations are carried out in the rest frame of the three-body system, and the internal momenta of the states will be described by the Jacobi variables $|\mathbf{p},\mathbf{q}\rangle_i$. For the particular case where the spectator is particle 1, the Jacobi variables are

$$\mathbf{p}=\mu(N_z)\left[\frac{\mathbf{k}_2}{m(n_{2z})}-\frac{\mathbf{k}_3}{m(n_{3z})}\right] , \qquad \mathbf{q}=\mathbf{k}_1=-(\mathbf{k}_2+\mathbf{k}_3) . \tag{12}$$

The partial-wave basis states in the J-j coupling scheme are abbreviated by

$$|pq\alpha\rangle_1=|pq(\{(LS)J,[ls(n_z)]j\}\mathcal{J}\mathcal{J}_z;[Tt(n_z)]\mathcal{T}\mathcal{T}_z;NN_z,\tfrac{1}{2}n_z)\rangle_1 , \tag{13}$$

which defines the set of quantum numbers α. In Eq. (13) the spectator, pair, and total quantum numbers are denoted by lower-case, upper-case, and script letters, respectively.

The three-body Hamiltonian H is

$$H=H_0+V , \tag{14}$$

where

$$V=V_1+V_2+V_3 \tag{15}$$

and V_i is the interaction between particles j and k

$$V_i=V_{jk}, \quad j\neq i\neq k\neq j . \tag{16}$$

The operator H_0 is the free, three-body Hamiltonian. The basis states $|pq\alpha\rangle_1$ of Eq. (13) are eigenstates of H_0:

$$H_0|pq\alpha\rangle_1=\left[[M(N_z)+m(n_z)]c^2+\frac{\hbar^2q^2}{2m(n_z)}+\frac{\hbar^2q^2}{2M(N_z)}+\frac{\hbar^2p^2}{2\mu(N_z)}\right]|pq\alpha\rangle_1 . \tag{17}$$

The meanings of the various terms are self-evident. The q^2-dependent terms—the kinetic energy of the spectator particle in the three-body center of mass, and the kinetic energy of the motion of the pair center of mass (again in the three-body center-of-mass system)—could obviously be combined into one term involving the reduced mass of the spectator-pair system. However, it proves useful to leave Eq. (17) as it stands (see Appendix B).

The three-body Hamiltonian is fully symmetric under exchange of any two particles. Since the nucleons-only (NNN) states must be antisymmetric under exchange of any two particles, the only states containing Δ's which can couple to them through the Hamiltonian are also necessarily antisymmetric under two-particle exchange. Formally, it is this fact that allows one to treat the nucleon and Δ as identical particles within the context of the generalized Pauli principle and to reduce the Faddeev equations from three components to one. This is accomplished in the practical solution of the Faddeev equations by restricting the two-body basis states to those for which $L+S+T+N$ is even [see Eq. (11)].

The formal Faddeev equation for the bound state of three identical particles can then be written succinctly as

$$|\Psi\rangle_1=t_1(E)(P_a+P_c)G_0(E)|\Psi\rangle_1 , \tag{18}$$

where $|\Psi\rangle_1$ is the Faddeev amplitude for the case where particle 1 is the spectator, and is related to the full three-body bound-state wave function by

$$|\Psi_B\rangle=G_0(E)(e+P_a+P_c)|\Psi\rangle_1 . \tag{19}$$

The three-body operators e, P_c, and P_a are the identity, the cyclic permutation, and the anticyclic permutation operators, respectively. The free, three-body Green's function has its usual definition

$$G_0(E)=\frac{1}{E-H_0} , \tag{20}$$

and the operator $t_1(E)$ is a two-body t matrix embedded in the three-body space; $t_1(E)$ is defined as the solution of the Lippmann-Schwinger equation

$$t_1(E)=V_1+V_1G_0(E)t_1(E) . \tag{21}$$

The operator $t_1(E)$ is discussed in more detail in Appendix B. The parametric energy E which appears in Eqs. (18)–(21) is the energy of the three-body bound state, which in the three-body center of mass is simply the rest-mass energy of the triton,

$$E = M_T c^2 \tag{22}$$

$$\equiv 3M_N c^2 - E_T \ , \tag{23}$$

where the last equation defines the binding energy E_T. Since all the particles are being treated as identical, the subscript on the basis states, Faddeev amplitudes, etc., is unnecessary and can be dropped.

Taking the projection of the Faddeev amplitude onto the three-body basis states

$$\Psi(pq\alpha) = \langle pq\alpha | \Psi \rangle \tag{24}$$

leads to the coupled set of integral equations

$$\Psi(pq\alpha) = \sum_{\bar{\gamma}} \sum_{\alpha'} \int_0^\infty dq' q'^2 \int_{-1}^{1} dx' t^{JT}_{\gamma,\bar{\gamma}}(p,p_1;E,q,n_z) \times \frac{G_{\bar{\alpha},\alpha'}(q,q',x')\Psi(p_2,q',\alpha')}{E - [m(n_z')+M(N_z')]c^2 - [\hbar^2 q'^2/2m(n_z')] - [\hbar^2 q'^2/2M(N_z')] - [\hbar^2 p_2^2/2\mu(N_z')]} \ , \tag{25}$$

where

$$x' = \frac{\mathbf{q}\cdot\mathbf{q}'}{qq'} \ . \tag{26}$$

The notation here is

$$\gamma = \{LSNN_z\} \ , \tag{27}$$

$$\bar{\gamma} = \{\overline{LSNN_z}\} \ , \tag{28}$$

$$\bar{\alpha} = (\{(\overline{LS})J, [ls(n_z)]j\}\mathcal{J}\mathcal{J}_z; [Tt(n_z)]\mathcal{T}\mathcal{T}_z; \overline{NN_z}, \tfrac{1}{2}n_z) . \tag{29}$$

Note that $\bar{\alpha}$ differs from α only through the substitution of the quantum numbers $\bar{\gamma}$ for γ. The quantity $G_{\bar{\alpha},\alpha'}(q,q',x')$ is just the usual geometrical coefficient, generalized to allow any number of Δ's, and is given in Appendix A. The variables p_1 and p_2 which appear in Eq. (25) are given by

$$p_1^2 = \left[\frac{m(n_z')}{M(\bar{N}_z)}\right]^2 q^2 + q'^2 + 2\left[\frac{m(n_z')}{M(\bar{N}_z)}\right] qq'x' \tag{30}$$

and

$$p_2^2 = q^2 + \left[\frac{m(n_z)}{M(N_z')}\right]^2 q'^2 + 2\left[\frac{m(n_z)}{M(N_z')}\right] qq'x' \ , \tag{31}$$

respectively. One important complication in Eq. (25) is the dependence of the variable p_1 on n_z', the spectator quantum number associated with the Faddeev component on the right-hand side of this equation. This is the only dependence of the t matrices on the α' quantum numbers. However, the operator $t_1(E)$ of Eq. (21) does depend in a nontrivial way on the spectator quantum number n_z, through the $m(n_z)$ which appears in the spectator kinetic-energy operator in $G_0(E)$. This leads, in the case where the spectator is a Δ, to a shift in the energy available to the pair by an amount proportional to the $N\Delta$ mass difference (see Appendix B). Equation (25) is the Faddeev equation which is solved for the triton binding energy E_T.

For the purpose of classifying three-body calculations, it has become customary to refer to the number of three-body "channels," where a "channel" corresponds to a unique set of quantum numbers α [see Eq. (13)]. In this work, it is useful to distinguish between two-body "channels" and two-body "amplitudes." In what follows, a two-body "channel" shall be determined by the unique set of two-body quantum numbers $\{J,T,\gamma\}$, i.e., $\{J,T,L,S,N,N_z\}$, while reference to a two-body "amplitude" shall always imply a unique set of quantum numbers $\{J,T,\gamma,\gamma'\}$.

III. FORCE MODEL

In this section, the potential used in the three-body Hamiltonian, Eq. (14), is given. To fully identify a given partial-wave amplitude of a two-body potential in the notation introduced in the preceding section, one writes $V^{JT}_{\gamma,\gamma'}$ with γ defined in Eq. (27). Because the use of N spin is unfamiliar in the present context, the potential matrix element $V^{JT}_{\gamma,\gamma'}$ for the transition potential from an NN state to an $N\Delta$ state is expressed here in terms of (particle-label) unsymmetrized $N\Delta$ states, through the use of Eqs. (7) and (11):

$$V(p,p')^{JT}_{LSN(N_z=0);L'S'(N'=1)(N_z'=-1)}$$

$$= \frac{1}{\sqrt{2}}(\langle p\{[L(\tfrac{3}{2},\tfrac{1}{2})S]JT\}(\Delta N)|V|p'\{[L'(\tfrac{1}{2},\tfrac{1}{2})S']JT\}(NN)\rangle$$

$$-(-1)^N\langle p\{[L(\tfrac{1}{2},\tfrac{3}{2})S]JT\}(N\Delta)|V|p'\{[L'(\tfrac{1}{2},\tfrac{1}{2})S']JT\}(NN)\rangle)$$

$$= \sqrt{2}\langle p\{[L(\tfrac{3}{2},\tfrac{1}{2})S]JT\}(\Delta N)|V|p'\{[L'(\tfrac{1}{2},\tfrac{1}{2})S']JT\}(NN)\rangle \ . \tag{32}$$

The $N\Delta$ states which appear on the right-hand side of this equation are not symmetrized, and the particle ordering is therefore relevant. The NN states in the n-spin notation are exactly the same as in the more conventional notation, and so the potential amplitudes for NN-NN transitions are just the usual ones. One should note that the quantum numbers denoted by γ are just those which are not conserved by the potential. Thus, N (as well as N_z) need not be conserved. To simplify the discussion in the remainder of this section, all quantum numbers other than N_z will be suppressed, and the notation $V^{n_z}_{N_z,N_z'}$ is introduced. The superscript identifies the nucleonic state of the "spectator" particle, i.e., the particle in the triton which is not participating in the interaction. The reason for this unusual notation will be made evident shortly.

The force models used in this work are based on those defined by the Hannover group [25]:

$$V_{N_z,N_z'}=\begin{cases} V_{-1,-1}, & NN\text{-}NN, \\ V_{-1,0}, & NN\text{-}N\Delta, \\ V_{0,-1}, & N\Delta\text{-}NN. \end{cases} \tag{33}$$

The potential $V_{0,0}$ (both direct and exchange terms), as well as all potentials with more than one Δ in either the initial or final state, are defined to be zero. The NN-NN potential is defined in terms of the NN-$N\Delta$ potential via the equation

$$V_{-1,-1}=V_P-V_{-1,0}g_0(E_r)V_{0,-1}\ . \tag{34}$$

Here V_P denotes the Paris [6] NN potential, and g_0 is the two-body Green's function

$$g_0(E)=\frac{1}{E-h_0}\ . \tag{35}$$

This choice of the NN-NN potential ensures that the resulting NN-NN t matrix will agree exactly with the Paris NN t matrix at the "renormalization" energy, E_r. Specifically, the NN-NN t matrices of the Hannover models are identical to those which result from the NN-NN energy-dependent effective potential

$$\begin{aligned} V_{\rm eff}(E)&=V_{-1,-1}+V_{-1,0}g_0(E)V_{0,-1} \\ &=V_P+V_{-1,0}[g_0(E)-g_0(E_r)]V_{0,-1} \end{aligned} \tag{36}$$

and no explicit coupling between NN and $N\Delta$ channels. In Ref. [25], E_r is chosen such that the relative energy in the two-nucleon center-of-mass system is zero. With the definition of h_0 in Eq. (8), the corresponding E_r is given here by twice the nucleon rest-mass energy, $2M_Nc^2$.

There are two conceivable, alternative definitions for the NN-$N\Delta$ potential $V^{n_z}_{-1,0}$. The first, more conventional, choice is independent of the state of the spectator particle, and leads to

$$\begin{aligned} V^{n_z}_{-1,-1}&=V_{-1,-1}\ , \\ V^{n_z}_{-1,0}&=V_{-1,0}\ , \end{aligned} \tag{37}$$

for both $n_z=\pm\frac{1}{2}$. A second alternative is to define

$$V^{n_z}_{-1,0}=\begin{cases} V_{-1,0}, & n_z=-\frac{1}{2}, \\ 0, & n_z=+\frac{1}{2}, \end{cases} \tag{38}$$

so that the NN-NN potential which follows from Eq. (34) is

$$V^{n_z}_{-1,-1}=\begin{cases} V_P-V_{-1,0}g_0(E_r)V_{0,-1}, & n_z=-\frac{1}{2}, \\ V_P, & n_z=+\frac{1}{2}. \end{cases} \tag{39}$$

This second alternative effectively restricts the three-body Hilbert space to the nucleons-only states plus those three-body states with only one Δ. When the spectator particle is a Δ, then the pair (which must be nucleons) is never able to make a transition to a $N\Delta$ state due to the fact that $V^{1/2}_{-1,0}=0$. The first alternative, on the other hand, allows intermediate one-Δ states in the two-body system to influence the NN-NN t matrices even when the spectator is a Δ, since $V^{1/2}_{-1,0}=V_{-1,0}$. For either alternative, the three-body channels which actually appear in the Faddeev equation, Eq. (25), are those that contain, at most, one Δ. Both alternatives will be considered in the present work [28]. The first definition will be called the "Hannover" (H) model, and the second will be referred to as the "Hannover*" (H^*) model. The H and H^* models are discussed in more detail in Sec. IV.

The transition potential $V_{0,-1}$ contains contributions from both π and ρ exchanges. In momentum and coordinate space, these contributions in terms of unsymmetrized $N\Delta$ states [see Eq. (32)] are

$$\langle \mathbf{p}|V_{N\Delta,NN}(\pi,m)|\mathbf{p}'\rangle=-\frac{1}{(2\pi\hbar)^3}\frac{f_{\pi NN}f_{\pi N\Delta}}{m_\pi^2c^4}\frac{\Lambda^2-m_\pi^2c^2}{\Lambda^2+(\mathbf{p}-\mathbf{p}')^2}\tau_2\cdot\mathbf{T}_3\frac{\sigma_2\cdot(\mathbf{p}-\mathbf{p}')\mathbf{S}_3\cdot(\mathbf{p}-\mathbf{p}')}{m^2c^2+(\mathbf{p}-\mathbf{p}')^2}\ , \tag{40}$$

$$\langle \mathbf{p}|V_{N\Delta,NN}(\rho,m)|\mathbf{p}'\rangle=-\frac{1}{(2\pi\hbar)^3}\frac{f_{\rho NN}f_{\rho N\Delta}}{m_\rho^2c^4}\frac{\Lambda^2-m_\rho^2c^2}{\Lambda^2+(\mathbf{p}-\mathbf{p}')^2}\tau_2\cdot\mathbf{T}_3\frac{[\sigma_2\times(\mathbf{p}-\mathbf{p}')]\cdot[\mathbf{S}_3\times(\mathbf{p}-\mathbf{p}')]}{m^2c^2+(\mathbf{p}-\mathbf{p}')^2}\ , \tag{41}$$

$$\begin{aligned} \langle \mathbf{r}|V_{N\Delta,NN}(\pi,m)|\mathbf{r}'\rangle=\delta^3(\mathbf{r}-\mathbf{r}')\tau_2\cdot\mathbf{T}_3\frac{f_{\pi NN}f_{\pi N\Delta}}{4\pi m_\pi^2c^4}\frac{\Lambda^2-m_\pi^2c^2}{\Lambda^2-m^2c^2}\left\{\frac{1}{3}\sigma_2\cdot\mathbf{S}_3\left[m^3c^6Y\left[\frac{mc}{\hbar}r\right]-\Lambda^3c^3Y\left[\frac{\Lambda}{\hbar}r\right]\right]\right. \\ \left.+\frac{1}{3}S_{23}\left[m^3c^6T\left[\frac{mc}{\hbar}r\right]-\Lambda^3c^3T\left[\frac{\Lambda}{\hbar}r\right]\right]\right\}\ , \end{aligned} \tag{42}$$

$$\langle \mathbf{r}|V_{N\Delta,NN}(\rho,m)|\mathbf{r}'\rangle=\delta^3(\mathbf{r}-\mathbf{r}')\tau_2\cdot\mathbf{T}_3\frac{f_{\rho NN}f_{\rho N\Delta}}{4\pi m_\rho^2c^4}\frac{\Lambda^2-m_\rho^2c^2}{\Lambda^2-m^2c^2}\left\{\frac{2}{3}\sigma_2\cdot\mathbf{S}_3\left[m^3c^6Y\left[\frac{mc}{\hbar}r\right]-\Lambda^3c^3Y\left[\frac{\Lambda}{\hbar}r\right]\right]\right.$$
$$\left.-\frac{1}{3}S_{23}\left[m^3c^6T\left[\frac{mc}{\hbar}r\right]-\Lambda^3c^3T\left[\frac{\Lambda}{\hbar}r\right]\right]\right\}, \quad (43)$$

where

$$S_{23}=3\sigma_2\cdot\hat{r}\mathbf{S}_3\cdot\hat{r}-\sigma_2\cdot\mathbf{S}_3\ , \quad (44)$$

$$Y(x)=\frac{e^{-x}}{x}\ , \quad (45)$$

$$T(x)=\left[1+\frac{3}{x}+\frac{3}{x^2}\right]Y(x)\ . \quad (46)$$

Also, in Eqs. (40)–(43), σ_i (τ_i) is the spin (isospin) operator in the spin-$\frac{1}{2}$ representation, and $\mathbf{S}_i$ ($\mathbf{T}_i$) is the $\frac{1}{2}$ to $\frac{3}{2}$ spin (isospin) transition operator. The matrix elements of the coordinate-space operators appearing in Eqs. (42) and (43) can be evaluated using standard angular momentum techniques [29] with the results [7], using Edmond's convention [30,31] for the reduced matrix elements,

$$\langle(s_2s_3)SS_z|\sigma_2\cdot\mathbf{S}_3|(s_2's_3')S'S_z'\rangle=(-1)^{s_2'+s_3+S'}\delta_{SS'}\begin{Bmatrix}S' & s_3 & s_2\\ 1 & s_2' & s_3'\end{Bmatrix}(s_2||\sigma_2||s_2')(s_3||\mathbf{S}_3||s_3')\ , \quad (47)$$

$$\langle\{L(s_2s_3)S\}J|S_{23}|\{L'(s_2's_3')S'\}J\rangle=(-1)^{S+J}[30(2L+1)(2L'+1)(2S+1)(2S'+1)]^{1/2}$$
$$\times\begin{Bmatrix}J & S & L\\ 2 & L' & S'\end{Bmatrix}\begin{bmatrix}L & 2 & L'\\ 0 & 0 & 0\end{bmatrix}\begin{Bmatrix}s_2 & s_2' & 1\\ s_3 & s_3' & 1\\ S & S' & 2\end{Bmatrix}(s_2\|\sigma_2\|s_2')(s_3\|\mathbf{S}_3\|s_3') \quad (48)$$

with an expression similar to Eq. (47) for the isospin. In Eqs. (47) and (48), the reduced matrix elements are $(\frac{1}{2}\|\sigma\|\frac{1}{2})=\sqrt{6}$ and $(\frac{3}{2}\|\mathbf{S}\|\frac{1}{2})=2$. Table I summarizes the physical constants used in the evaluation of the potential, which have been chosen for compatibility with those employed in Refs. [25] and [27]. The N and Δ masses used are 938.93 and 1236 MeV, respectively.

Two different forms for the NN-$N\Delta$ potential are defined in Ref. [25] and shall be labeled as $H1$ and $H2$. Potential $H1$ is given by

$$V_{0,-1}=\sum_{\alpha=\pi,\rho}V_{0,-1}(\alpha,m_\alpha)\ . \quad (49)$$

The second potential, $H2$, is

$$V_{0,-1}=\tfrac{1}{2}\sum_{\alpha=\pi,\rho}[V_{0,-1}(\alpha,m_\alpha)+V_{0,-1}(\alpha,\sqrt{m_\alpha(m_\alpha+M_\Delta-M_N)})]\ . \quad (50)$$

Of importance in assessing the physical relevance of the Hannover one-Δ models is their performance in describing the low-energy scattering parameters of the two-body system. First, the characterization of the Hannover $H1$ and $H2$ models as summarized in Ref. [25] is that the $^1S_0$ scattering length and effective range differ from those of the Paris potential by less than 0.1 fm and by less than 0.01 fm, respectively, and that all phase shifts are within 1° of the Paris potential values from threshold to $E_{\rm lab}=100$ MeV. Our own investigations differ with each of these characterizations. For the scattering length we find that the $H1$, $H2$, and Paris values are identical (-17.55 fm for np scattering). In fact, the equality of the scattering lengths can be demonstrated analytically by an effective-range-type analysis based on the potentials V_P and $V_{\rm eff}$. Labeling quantities which correspond to V_P and $V_{\rm eff}$ by subscripts P and e, respectively, and writing for the $^1S_0$ scattering wave functions $\psi=v/r$, with v asymptotic to $\sin(kr+\delta)/\sin(\delta)$, one finds

$$k\cot\delta_e-k\cot\delta_P=\frac{2\mu}{\hbar^2}\int_0^\infty dr\,v_P(r)[V_{\rm eff}-V_P]v_e(r)$$
$$=\frac{2\mu}{\hbar^2}\int_0^\infty dr\,v_P(r)\{V_{-1,0}[g_0(E)-g_0(E_r)]V_{0,-1}\}v_e(r)\ . \quad (51)$$

TABLE I. Values of the potential parameters as used in this work.

Parameter	Value
$f^2_{\pi NN}/4\pi$	0.08
$f^2_{\pi N\Delta}/4\pi$	0.35
$f^2_{\rho NN}/4\pi$	5.20
$f^2_{\rho N\Delta}/4\pi$	22.8
$m_\pi c^2$	138.0 MeV
$m_\rho c^2$	760.0 MeV
Λc	1.2 GeV

Since the lowest-order term of the right-hand side of Eq. (51) is $O(k^2)$, while the left-hand side can be rewritten directly in terms of the effective-range expansions for $k\cot\delta_e$ and $k\cot\delta_P$, the equality of the two scattering lengths is immediate. For the effective range we find (again for the *np* case) the values 2.86, 2.75, and 2.76 fm for the Paris, $H1$, and $H2$ models, respectively. That the effective ranges of the Hannover models lie below the Paris value also follows from Eq. (51). Our results for the Paris potential are in good agreement with those given in Ref. [32], while our differences with Ref. [25] regarding the comparison of the Paris and $H1$ scattering lengths and effective ranges are in accord with similar discrepancies noted in Ref. [27]. The deviation of the effective ranges in the Hannover models from the Paris value is substantial both relative to the accuracy with which this parameter is known and relative to the scale set by its impact on the triton, the triton binding being much more sensitive to variation of the effective range than to variation of the scattering length [33,34]. In fact, using the scale set by Refs. [33] and [34], the decreased effective range of the Hannover models corresponds to an unwarranted increase in the triton binding of about 200 keV. Finally, we are in agreement with the phase-shift characterization of Ref. [25] for all channels except the $^1S_0$. For this channel, however, we find substantially larger phase shifts for the Hannover models than for the Paris potential, with the phase shifts differing by about 1.5° and 3° at $E_{\rm lab}=25$ and 100 MeV, respectively. The enhanced $^1S_0$ phase shifts of the Hannover models are, of course, consistent with their reduced $^1S_0$ effective ranges.

The differences found between the $^1S_0$ predictions of the Paris and Hannover models, and to a lesser extent phase-shift differences observed in the three ^3P channels below $E_{\rm lab}=100$ MeV, are substantial and must be regarded as defects of the Hannover one-Δ models. This is especially true of the $^1S_0$ discrepancies, since this channel plays such an important role in the triton. In fact, the estimated 200 keV increase in triton binding that goes along with the unwarranted reduction of the $^1S_0$ effective range in the Hannover models represents a large fraction of the net effect ultimately attributed to the Δ degrees of freedom in these models [25].

Second, the renormalization and its associated energy, E_r, clearly play an important role in the Hannover models. In fact, the triton calculations of Ref. [25] found a large, repulsive contribution to the triton binding energy from dispersive effects associated directly with the energy dependence of $V_{\rm eff}$. This can be understood using a simple, schematic examination of the second term of Eq. (36). This term can be approximated as $-V_{-1,0}(E-E_r)V_{0,-1}/(\Delta M)^2$, where ΔM represents the Δ-nucleon mass difference. For $V_{-1,0}$ of order 50 MeV and ΔM of order 300 MeV, this becomes simply $(E_r-E)/36$. Taking E_r to be at threshold implies that this term makes no contribution to the potential at threshold. However, taking the average energy relevant to triton calculations to be 20 MeV below threshold (see Ref. [11]) then yields a repulsive contribution of about 555 keV, very close to what is found from a detailed three-body calculation (see Ref. [25] or Sec. IV). Within this schematic picture, the cogency of which is borne out by actual triton calculations varying E_r, it is clear that the dispersive effect seen in the triton binding is very sensitive to the value of E_r.

Since the dispersive effect is large, and since it is sensitive to the energy E_r at which the subtraction in Eq. (36) is made, it is crucial to the physical relevance of the Hannover models that E_r be closely determined by some aspect of the two-body scattering data. This consistency criterion turns out to be nicely fulfilled: although the effective range is relatively insensitive to the choice of E_r, the scattering length varies rapidly with changing E_r, both of which are expected on the basis of the simple schematic picture. For the $H1$ model, the scattering length at $E_r-2M_Nc^2=-4.0$, -1.0, 0.0, 1.0, and 4.0 MeV is -19.13, -17.93, -17.55, -17.19, and -16.18 fm. The behavior of the $H2$ model is similar. From this we conclude that in the Hannover one-Δ models the value of E_r, and thus the size of the repulsive dispersive effect, is strongly constrained by the necessity to leave the $^1S_0$ scattering length unchanged. Thus, the Hannover one-Δ models are well motivated in those aspects related to the $^1S_0$ scattering length, whereas energy-dependent effects, most notably those related to the $^1S_0$ effective range, are more problematical.

IV. RESULTS

The two-body channels which form the basis for the calculations reported in this paper are those which contain, at most, one Δ resonance and have total angular momentum $J\leq 4$. Channels containing a Δ are also restricted to have total orbital angular momentum $L(N\Delta)\leq 4$. The corresponding three-body channels are all of those that can be built from these two-body channels and contain at most one Δ. Because the Hannover potential model has no interaction between nucleon-delta $(N\Delta)$ states, those $N\Delta$ states which decouple from the NN sector have vanishing two-body amplitudes (t matrices) and are thus eliminated from the list of two-body channels and from the construction of the three-body channels. These include all $(N\Delta)$ states with $(J=1, T=1, \pi=+)$ or $(J=3, T=1, \pi=+)$, where π signifies parity. In addition, since the tensor force allows no spin-singlet to spin-triplet transitions, the $^3D_2$ and $^3G_4$ $N\Delta$ states also decouple from the NN sector and are eliminated.

Although there is no force connecting $N\Delta$ states in the Hannover potential model, two-body amplitudes between $N\Delta$ states need not be neglected (set to zero) in the solution of the three-body bound-state problem. Nonzero two-body amplitudes between $N\Delta$ states arise from the solution of the two-body Lippmann-Schwinger equation, and these amplitudes can be included in the solution of the Faddeev equation. Consistent with the above restrictions on the two-body channels, there are a total of 129 nonzero two-body transition amplitudes between 37 distinct two-body channels, from which 103 three-body channels containing, at most, a single Δ can be constructed.

This represents a formidable nuclear three-body problem, far more extensive than has previously been solved. It is thus useful, both technically and in the interest of sorting out the contributions of various physical components, to subdivide the problem and build up the full analysis from its component parts. This allows close contact with the previous work and provides better insight into the implications of the full solution, as well as proving useful as a matter of economy. The two-body channels can be divided into 22 channels with $J \leq 2$ and 15 channels with $J = 3,4$. For $J \leq 2$, the 22 channels can be further divided into two sets, the 4 channels involving an $N\Delta$ state with $L(N\Delta) \geq 3$ and the remaining 18 channels. These 18 two-body channels have $J \leq 2$, at most one Δ, and do not involve an $N\Delta$ pair with $L(N\Delta) \geq 3$; i.e., they are the channels used in the original Hannover calculations. It is convenient to similarly divide the $J \geq 3$ two-body channels into two sets, the 5 channels involving an $N\Delta$ state with $L(N\Delta) \geq 3$ and the remaining 10. The 10-channel set is the natural extension of the Hannover truncation scheme from $J \leq 2$ to $J \leq 4$.

The three-body channels are also subdivided in a manner which allows close contact with the original Hannover calculations. First, the 103 three-body channels are divided into two groups, 57 channels with $J \leq 2$ and 46 channels with $J = 3,4$. Each of these groups is then divided into three sets of channels: one set consists of those channels containing an $N\Delta$ pair with $L(N\Delta) \geq 3$, one set consists of all those channels which have a Δ spectator and a nucleon pair in a state other than $^1S_0$, and the third set contains the remaining channels. For $J \leq 2$ this yields 8, 16, and 33 channels, respectively. The 33-channel set is just the set originally employed in the Hannover calculations. For $J = 3,4$ the three sets contain 10, 16, and 20 channels, respectively. The 20-channel set is the natural extension of the Hannover three-body truncation scheme from (pair) $J \leq 2$ to $J \leq 4$.

For ease of reference the two- and three-body channels are collected in Tables II–VIII. Tables II–IV display the two-body channels; Tables V–VIII hold the three-body channels. Table II contains the set of 18 two-body channels of the original Hannover calculation, while Table III contains the remaining 4 two-body channels present for $J \leq 2$. Table IV contains the $J = 3,4$ channels, subdivided as described above. Table V contains the 33 three-body channels of the original Hannover calculation, while Table VI contains the remaining 24 $J \leq 2$ three-body channels, subdivided as described above. Table VII holds the 20 three-body channels which extend the Hannover scheme to $J \leq 4$, and Table VIII contains the remaining 26 three-body channels, also subdivided as described above.

This division of the two- and three-body channels corresponds to the pattern of our investigation of the full one-Δ problem. Restricting the included channels to $J \leq 2$, we first examine the problem within the context of the original Hannover channel-truncation scheme, i.e., within the confines of the 18 two-body channels of Table II and the 33 three-body channels of Table V. Because of its importance, this part of the problem is examined in considerable detail. Then, the effect of the 16 Δ-spectator channels of Table VI is determined by a 49-channel calculation. Finally, the $L(N\Delta) \geq 3$ channels of Tables III

TABLE II. The 18 two-body channels of the original Hannover calculation.

No.	J	T	L	S	N	N_z
1	0	1	0	0	1	−1
2	0	1	2	2	1	0
3	0	1	1	1	1	−1
4	0	1	1	1	1	0
5	1	0	0	1	1	−1
6	1	0	2	1	1	−1
7	1	0	1	0	1	−1
8	1	1	1	1	1	−1
9	1	1	1	1	1	0
10	1	1	1	2	0	0
11	2	0	2	1	1	−1
12	2	1	2	0	1	−1
13	2	1	0	2	1	0
14	2	1	2	2	1	0
15	2	1	1	1	1	−1
16	2	1	3	1	1	−1
17	2	1	1	1	1	0
18	2	1	1	2	0	0

TABLE III. The four additional two-body channels for $J \leq 2$.

No.	J	T	L	S	N	N_z
1	1	1	3	2	0	0
2	2	1	4	2	1	0
3	2	1	3	1	1	0
4	2	1	3	2	0	0

and VI are incorporated, yielding a total of 57 three-body channels.

Next, an analogous development is used to treat the channels with $J=3,4$. Allowing all the nucleons-only channels but only those Δ channels with either $L(N\Delta)\leq 2$ or a spectator Δ coupled to the $^1S_0(NN)$ state yields the natural extension of the Hannover truncation scheme to $J\leq 4$. This system encompasses the $(18+10=28)$ two-body channels of Tables II and IV, and the $(33+20=53)$ three-body channels of Tables V and VII. Subsequently, the 32 Δ-spectator channels of Tables VI and VIII are included to form an 85-channel three-body system. Finally, the $L(N\Delta)\geq 3$ channels of Tables III and IV, and Tables VI and VIII, are incorporated to complete the full set of 103 channels.

The Faddeev calculations reported in this paper fall broadly into four distinct dynamical categories: (1) Standard nucleons-only calculations based on the Paris NN potential, denoted "Paris"; (2) calculations which use the Hannover $H1$ or $H2$ force models in the two-body system, with the three-body channels being those (with at most one Δ) built from the employed two-body channels. This category is further divided into calculations of two types, those which neglect two-body amplitudes between $N\Delta$ channels, denoted $HA1$ or $HA2$ (or generically HA), and those which do not, denoted $HB1$ or $HB2$ (or generically HB); (3) a variation on the preceding category in which the Hannover $H1$ or $H2$ two-body amplitudes are replaced (in the Faddeev calculation) by the analogous Paris amplitudes when the spectator particle is a Δ, denoted $HA1^*$ or $HA2^*$, or generically HA^* (or $HB1^*$, $HB2^*$, or generically HB^*, depending on the neglect or inclusion of two-body amplitudes between $N\Delta$ channels); (4) calculations using the Hannover $H1$ or $H2$ force models to determine the two-body amplitudes, but then allowing only nucleons (and hence using only NN-NN two-body amplitudes) in the three-body system, termed "dispersive" and denoted DISP. Dispersive results, of course, depend on the $N\Delta$ channels allowed to contribute to the determination of the NN-NN amplitudes. All results denoted DISP, or referred to as "dispersive," without qualification, restrict $L(N\Delta)\leq 2$. Dispersive results which incorporate $L(N\Delta)=3,4$ are also important and will be explicitly identified when needed.

The calculations of categories (1)–(3) maintain a special consistency between the truncation schemes used in the two- and three-body systems, in that all of the channels included in the solution of the two-body Lippmann-Schwinger equation also appear explicitly in the three-body channels included in the solution of the Faddeev equation, subject only to the restriction that the three-body channels contain at most one Δ. Thus, two-body dispersive and three-body-force effects are included on the same footing. This is important because these two effects were found in [25] to be large but opposite in sign and largely offsetting. An inconsistent channel-truncation scheme prejudices the result by emphasizing one type of effect over the other.

The calculations of category (3) take the foregoing consistency a step further than those of category (2) by

TABLE IV. The 15 two-body channels for $J=3,4$: first the 10-channel extension of the Hannover truncation scheme, then the 5 channels involving $L(N\Delta)\geq 3$.

No.	J	T	L	S	N	N_z
1	3	0	2	1	1	−1
2	3	0	4	1	1	−1
3	3	0	3	0	1	−1
4	3	1	3	1	1	−1
5	3	1	1	2	0	0
6	4	0	4	1	1	−1
7	4	1	4	0	1	−1
8	4	1	2	2	1	0
9	4	1	3	1	1	−1
10	4	1	5	1	1	−1
1	3	1	3	1	1	0
2	3	1	3	2	0	0
3	4	1	4	2	1	0
4	4	1	3	1	1	0
5	4	1	3	2	0	0

TABLE V. The 33 three-body channels of the original Hannover calculation.

No.	J	T	L	S	N	N_z	l	j	n_z
1	0	1	0	0	1	−1	0	$\frac{1}{2}$	$-\frac{1}{2}$
2	0	1	0	0	1	−1	2	$\frac{1}{2}$	$\frac{1}{2}$
3	0	1	2	2	1	0	0	$\frac{1}{2}$	$-\frac{1}{2}$
4	0	1	1	1	1	−1	1	$\frac{1}{2}$	$-\frac{1}{2}$
5	0	1	1	1	1	0	1	$\frac{1}{2}$	$-\frac{1}{2}$
6	1	0	0	1	1	−1	0	$\frac{1}{2}$	$-\frac{1}{2}$
7	1	0	0	1	1	−1	2	$\frac{3}{2}$	$-\frac{1}{2}$
8	1	0	2	1	1	−1	0	$\frac{1}{2}$	$-\frac{1}{2}$
9	1	0	2	1	1	−1	2	$\frac{3}{2}$	$-\frac{1}{2}$
10	1	0	1	0	1	−1	1	$\frac{1}{2}$	$-\frac{1}{2}$
11	1	0	1	0	1	−1	1	$\frac{3}{2}$	$-\frac{1}{2}$
12	1	1	1	1	1	−1	1	$\frac{1}{2}$	$-\frac{1}{2}$
13	1	1	1	1	1	−1	1	$\frac{3}{2}$	$-\frac{1}{2}$
14	1	1	1	1	1	0	1	$\frac{1}{2}$	$-\frac{1}{2}$
15	1	1	1	1	1	0	1	$\frac{3}{2}$	$-\frac{1}{2}$
16	1	1	1	2	0	0	1	$\frac{1}{2}$	$-\frac{1}{2}$
17	1	1	1	2	0	0	1	$\frac{3}{2}$	$-\frac{1}{2}$
18	2	0	2	1	1	−1	2	$\frac{3}{2}$	$-\frac{1}{2}$
19	2	0	2	1	1	−1	2	$\frac{5}{2}$	$-\frac{1}{2}$
20	2	1	2	0	1	−1	2	$\frac{3}{2}$	$-\frac{1}{2}$
21	2	1	2	0	1	−1	2	$\frac{5}{2}$	$-\frac{1}{2}$
22	2	1	0	2	1	0	2	$\frac{3}{2}$	$-\frac{1}{2}$
23	2	1	0	2	1	0	2	$\frac{5}{2}$	$-\frac{1}{2}$
24	2	1	2	2	1	0	2	$\frac{3}{2}$	$-\frac{1}{2}$
25	2	1	2	2	1	0	2	$\frac{5}{2}$	$-\frac{1}{2}$
26	2	1	1	1	1	−1	1	$\frac{3}{2}$	$-\frac{1}{2}$
27	2	1	1	1	1	−1	3	$\frac{5}{2}$	$-\frac{1}{2}$
28	2	1	3	1	1	−1	1	$\frac{3}{2}$	$-\frac{1}{2}$
29	2	1	3	1	1	−1	3	$\frac{5}{2}$	$-\frac{1}{2}$
30	2	1	1	1	1	0	1	$\frac{3}{2}$	$-\frac{1}{2}$
31	2	1	1	1	1	0	3	$\frac{5}{2}$	$-\frac{1}{2}$
32	2	1	1	2	0	0	1	$\frac{3}{2}$	$-\frac{1}{2}$
33	2	1	1	2	0	0	3	$\frac{5}{2}$	$-\frac{1}{2}$

effectively restricting the Hilbert space of the three-body problem to the NNN and $NN\Delta$ subspaces. Because the three-body channels may contain, at most, one Δ, it is slightly inconsistent to allow coupling to $N\Delta$ states to influence the two-body amplitudes (dispersive effect) when the spectator particle is a Δ. This allows states containing two Δ's to contribute a dispersive effect to the three-body system. Keeping the dispersive and three-body-force effects of the channels on a strictly equal footing would thus require the introduction of three-body channels containing two Δ's. As shown shortly, the difference in the binding energies of categories (2) and (3) is small, so that the correction of category (3) is not an essential one. The calculations of category (4) are, of course, designed solely for the purpose of isolating the dispersive effect, the qualitative features of which follow from the effective potential of Eq. (36) and the simple schematic picture of Sec. III.

Three-body calculations which include the two-body amplitudes between $N\Delta$ channels (types HB or HB^*) are motivated by the fact that these amplitudes arise naturally from the adopted force model and also with an eye to future comparisons with results from more sophisticated models. Planned comparisons with force models which include coupling to $\Delta\Delta$ channels and/or coupling between $N\Delta$ channels more cleanly isolate the added sophistications if the present calculations incorporate the amplitudes between $N\Delta$ channels. On the other hand, the amplitudes between $N\Delta$ channels produced by the present force model are doubtless a poor approximation to reality, in any sense. After all, the leading (Born) term in the Lippmann-Schwinger equation for these amplitudes has been completely neglected. From this point of view, it seems preferable to discard these questionable

TABLE VI. The remaining 24 three-body channels for $J \leq 2$: first the 8 channels which involve $L(N\Delta) \geq 3$, then the 16 additional Δ-spectator channels.

No.	J	T	L	S	N	N_z	l	j	n_z
1	1	1	3	2	0	0	1	$\frac{1}{2}$	$-\frac{1}{2}$
2	1	1	3	2	0	0	1	$\frac{3}{2}$	$-\frac{1}{2}$
3	2	1	4	2	1	0	2	$\frac{3}{2}$	$-\frac{1}{2}$
4	2	1	4	2	1	0	2	$\frac{5}{2}$	$-\frac{1}{2}$
5	2	1	3	1	1	0	1	$\frac{3}{2}$	$-\frac{1}{2}$
6	2	1	3	1	1	0	3	$\frac{5}{2}$	$-\frac{1}{2}$
7	2	1	3	2	0	0	1	$\frac{3}{2}$	$-\frac{1}{2}$
8	2	1	3	2	0	0	3	$\frac{5}{2}$	$-\frac{1}{2}$
1	0	1	1	1	1	−1	1	$\frac{1}{2}$	$\frac{1}{2}$
2	1	1	1	1	1	−1	1	$\frac{1}{2}$	$\frac{1}{2}$
3	1	1	1	1	1	−1	1	$\frac{3}{2}$	$\frac{1}{2}$
4	1	1	1	1	1	−1	3	$\frac{3}{2}$	$\frac{1}{2}$
5	2	1	2	0	1	−1	0	$\frac{3}{2}$	$\frac{1}{2}$
6	2	1	2	0	1	−1	2	$\frac{3}{2}$	$\frac{1}{2}$
7	2	1	2	0	1	−1	2	$\frac{5}{2}$	$\frac{1}{2}$
8	2	1	2	0	1	−1	4	$\frac{5}{2}$	$\frac{1}{2}$
9	2	1	1	1	1	−1	1	$\frac{3}{2}$	$\frac{1}{2}$
10	2	1	1	1	1	−1	3	$\frac{3}{2}$	$\frac{1}{2}$
11	2	1	1	1	1	−1	1	$\frac{5}{2}$	$\frac{1}{2}$
12	2	1	1	1	1	−1	3	$\frac{5}{2}$	$\frac{1}{2}$
13	2	1	3	1	1	−1	1	$\frac{3}{2}$	$\frac{1}{2}$
14	2	1	3	1	1	−1	3	$\frac{3}{2}$	$\frac{1}{2}$
15	2	1	3	1	1	−1	1	$\frac{5}{2}$	$\frac{1}{2}$
16	2	1	3	1	1	−1	3	$\frac{5}{2}$	$\frac{1}{2}$

TABLE VII. The 20 three-body channels which extend the Hannover truncation scheme to $J \leq 4$.

No.	J	T	L	S	N	N_z	l	j	n_z
1	3	0	2	1	1	−1	2	$\frac{5}{2}$	$-\frac{1}{2}$
2	3	0	2	1	1	−1	4	$\frac{7}{2}$	$-\frac{1}{2}$
3	3	0	4	1	1	−1	2	$\frac{5}{2}$	$-\frac{1}{2}$
4	3	0	4	1	1	−1	4	$\frac{7}{2}$	$-\frac{1}{2}$
5	3	0	3	0	1	−1	3	$\frac{5}{2}$	$-\frac{1}{2}$
6	3	0	3	0	1	−1	3	$\frac{7}{2}$	$-\frac{1}{2}$
7	3	1	3	1	1	−1	3	$\frac{5}{2}$	$-\frac{1}{2}$
8	3	1	3	1	1	−1	3	$\frac{7}{2}$	$-\frac{1}{2}$
9	3	1	1	2	0	0	3	$\frac{5}{2}$	$-\frac{1}{2}$
10	3	1	1	2	0	0	3	$\frac{7}{2}$	$-\frac{1}{2}$
11	4	0	4	1	1	−1	4	$\frac{7}{2}$	$-\frac{1}{2}$
12	4	0	4	1	1	−1	4	$\frac{9}{2}$	$-\frac{1}{2}$
13	4	1	4	0	1	−1	4	$\frac{7}{2}$	$-\frac{1}{2}$
14	4	1	4	0	1	−1	4	$\frac{9}{2}$	$-\frac{1}{2}$
15	4	1	2	2	1	0	4	$\frac{7}{2}$	$-\frac{1}{2}$
16	4	1	2	2	1	0	4	$\frac{9}{2}$	$-\frac{1}{2}$
17	4	1	3	1	1	−1	3	$\frac{7}{2}$	$-\frac{1}{2}$
18	4	1	3	1	1	−1	5	$\frac{9}{2}$	$-\frac{1}{2}$
19	4	1	5	1	1	−1	3	$\frac{7}{2}$	$-\frac{1}{2}$
20	4	1	5	1	1	−1	5	$\frac{9}{2}$	$-\frac{1}{2}$

TABLE VIII. The remaining 26 three-body channels for $J \leq 4$: first the 10 channels which involve $L(N\Delta) \geq 3$, then the 16 additional Δ-spectator channels.

No.	J	T	L	S	N	N_z	l	j	n_z
1	3	1	3	1	1	0	3	$\frac{5}{2}$	$-\frac{1}{2}$
2	3	1	3	1	1	0	3	$\frac{7}{2}$	$-\frac{1}{2}$
3	3	1	3	2	0	0	3	$\frac{5}{2}$	$-\frac{1}{2}$
4	3	1	3	2	0	0	3	$\frac{7}{2}$	$-\frac{1}{2}$
5	4	1	4	2	1	0	4	$\frac{7}{2}$	$-\frac{1}{2}$
6	4	1	4	2	1	0	4	$\frac{9}{2}$	$-\frac{1}{2}$
7	4	1	3	1	1	0	3	$\frac{7}{2}$	$-\frac{1}{2}$
8	4	1	3	1	1	0	5	$\frac{9}{2}$	$-\frac{1}{2}$
9	4	1	3	2	0	0	3	$\frac{7}{2}$	$-\frac{1}{2}$
10	4	1	3	2	0	0	5	$\frac{9}{2}$	$-\frac{1}{2}$
1	3	1	3	1	1	−1	1	$\frac{5}{2}$	$\frac{1}{2}$
2	3	1	3	1	1	−1	3	$\frac{5}{2}$	$\frac{1}{2}$
3	3	1	3	1	1	−1	3	$\frac{7}{2}$	$\frac{1}{2}$
4	3	1	3	1	1	−1	5	$\frac{7}{2}$	$\frac{1}{2}$
5	4	1	4	0	1	−1	2	$\frac{7}{2}$	$\frac{1}{2}$
6	4	1	4	0	1	−1	4	$\frac{7}{2}$	$\frac{1}{2}$
7	4	1	4	0	1	−1	4	$\frac{9}{2}$	$\frac{1}{2}$
8	4	1	4	0	1	−1	6	$\frac{9}{2}$	$\frac{1}{2}$
9	4	1	3	1	1	−1	3	$\frac{7}{2}$	$\frac{1}{2}$
10	4	1	3	1	1	−1	5	$\frac{7}{2}$	$\frac{1}{2}$
11	4	1	3	1	1	−1	3	$\frac{9}{2}$	$\frac{1}{2}$
12	4	1	3	1	1	−1	5	$\frac{9}{2}$	$\frac{1}{2}$
13	4	1	5	1	1	−1	3	$\frac{7}{2}$	$\frac{1}{2}$
14	4	1	5	1	1	−1	5	$\frac{7}{2}$	$\frac{1}{2}$
15	4	1	5	1	1	−1	3	$\frac{9}{2}$	$\frac{1}{2}$
16	4	1	5	1	1	−1	5	$\frac{9}{2}$	$\frac{1}{2}$

amplitudes (as in calculations HA or HA^*) and restrict the retained amplitudes to those that may more nearly reflect the actual physics present in the more realistic models. Since each type of calculation offers advantages, both have been included in this investigation. As seen shortly, it turns out that the two-body amplitudes connecting $N\Delta$ channels yield a small but significant increase in the triton binding energy.

Tables IX and X display results from 18-channel (18-ch) and 33-ch calculations in comparison with the corresponding values from Ref. [25]. Table IX holds binding-energy results, while Table X shows results for various components of the corresponding triton wave functions.

Several notable results are evident from Tables IX and X. The first one is our independent confirmation of the essential findings of the original Hannover $J \leq 2$ calculations [25]. Focusing on the triton binding, our values for the 18-ch DISP case are in substantial accord with those of Ref. [25], at least on the scale set by the size of the DISP effect itself. Similarly, our 33-ch HB^* results are close to the 33-ch results of Ref. [25]. The differences between our results and those of Ref. [25] are clearly inconsequential relative to assessing the basic physical implications of the one-Δ model, so that in this important regard our calculations confirm the earlier results of Ref. [25]. However, our differences with Ref. [25] are both numerically significant and non-negligible. We have gone to great lengths to ensure the reliability of our results; our efforts in this regard are summarized in Appendix C. Our numerical findings for the two-body scattering predictions of the Hannover one-Δ models are supported by the analytical effective range results of Sec. III, by their

TABLE IX. Selected results for the triton binding energy (MeV). Results from Ref. [25] are shown parenthetically. The 18-channel and 33-channel results are for $J \leq 2$, $\pi = \pm$.

Force	DISP (18-ch)	HA (33-ch)	HB (33-ch)	HA^* (33-ch)	HB^* (33-ch)
$H1$	6.83 (6.80)	7.70	7.77	7.74	7.82 (7.77)
$H2$	6.87 (6.80)	7.68	7.74	7.72	7.78 (7.72)

TABLE X. Wave-function probabilities for the Faddeev solutions corresponding to the calculations of Table IX. P_Δ denotes the Δ probability. P_S, P_P, and P_D denote S-, P-, and D-state probabilities, respectively, in the nucleons-only sector. Results from Ref. [25] are shown parenthetically for comparison.

Calculation	P_Δ (%)	P_S (%)	P_P (%)	P_D (%)
DISP ($H1$)		91.68	0.06	8.26
DISP ($H2$)		91.67	0.06	8.27
$HA1$ (33-ch)	2.21	88.95	0.10	8.74
$HA2$ (33-ch)	2.00	89.22	0.09	8.68
$HA1^*$ (33-ch)	2.23	88.91	0.10	8.76
$HA2^*$ (33-ch)	2.02	89.19	0.10	8.70
$HB1$ (33-ch)	2.34	88.81	0.10	8.75
$HB2$ (33-ch)	2.11	89.10	0.10	8.70
$HB1^*$ (33-ch)	2.37 (2.31)	88.76 (88.87)	0.10 (0.09)	8.77 (8.73)
$HB2^*$ (33-ch)	2.14 (2.33)	89.06 (88.92)	0.10 (0.09)	8.71 (8.66)

own internal consistency, and by the similar findings of Ref. [27], whereas the corresponding characterizations of Ref. [25] are at variance with these (see Sec. III). This is important because our disagreements with the three-body results of Ref. [25] are typified by the differences between the 18-ch DISP results, and these differences can only be due to disparity at the two-body level (because our three-body calculations for the 18-ch binding using the Paris potential agree with those of Ref. [25]). For these reasons we are confident of the accuracy and reliability of our numerics; this issue is especially important to us because of the extensions which are to be built on the present work. However, we emphasize that, non-negligible differences notwithstanding, our three-body results confirm the essential findings of the original Hannover three-body calculations.

Also evident from Tables IX and X is the fact that the difference between HA (HB) and HA^* (HB^*) results is very minor (40–50 keV for the binding energies), as might be expected since it depends for its existence on both a relatively small two-body dispersive effect and a small Δ-spectator component in the three-body wave function. This is important in that it indicates that our one-Δ results are not so fragile in regard to the neglect of two-Δ states as to be uninterpretable and because it enables us to restrict ourselves entirely to the more consistent HA^* and HB^* calculations in what follows. Similarly, comparison of the results for the $H1$ and $H2$ force models in Tables IX and X indicates that the two models are, for our purposes, equivalent. Thus, we need only consider one of the models in our further investigations. This is also evident in the results displayed in Table XI, which also shows some results from one-Δ calculations more restricted in nature than the full 33-channel one-Δ calculations. From this point on we consider exclusively the $H1$ force model, this choice being made because it is the $H1$ model which was previously extended to investigate two-Δ effects in the triton [26].

Finally, the large increase in binding energy evident in Table XI as the number of channels is increased, especially the increase in E_T in going from $J \leq 1$ (17-ch) to $J \leq 2$ (33-ch), suggests the need to examine contributions from $J \geq 3$, to find whether truncation at 33 channels is warranted or not.

The central results of our investigations are collected in Table XII. The main result is the 103-ch $HB1^*$ value for the triton binding energy, $E_T = 7.83$ MeV. Comparing this figure with the $J \leq 4$ Paris prediction, $E_T = 7.46$ MeV, gives the full one-Δ contribution to E_T as 370 keV. This number includes all one-Δ contributions with $L(N\Delta) \leq 4$, i.e., all the two-body channels of Tables II–IV and all the three-body channels of Tables V–VIII. Dispersive calculations which include the effect of the $L(N\Delta) = 3,4$ channels (not shown in Table XII) yield $E_T = 6.86$, 6.79, 6.92, and 6.63 MeV for the 34-, 18-, 9-, and 10-channel analogs of the DISP results of Table XII; comparing these figures to the corresponding values based on the Paris potential identifies the net repulsive effect as 600, 590, 490, and 470 keV. Thus, including the compensation of the 600 keV dispersive binding-energy loss, the net one-Δ three-body-force effect in the 103-ch result is about 970 keV.

One striking feature of Table XII is the near equality of the full 103-ch $HB1^*$ value for the triton binding, $E_T = 7.83$ MeV, and the corresponding 33-ch $HB1^*$

TABLE XI. Selected results for the triton binding energy. The 18-channel and 33-channel results are for $J \leq 2$, $\pi = \pm$. The 17-channel and 7-channel results are for $J \leq 1$, and for $\pi = \pm$ and $\pi = +$, respectively.

Force model	(18-ch) DISP	(7-ch) HA^*	(7-ch) HB^*	(17-ch) HA^*	(17-ch) HB^*	(33-ch) HA^*	(33-ch) HB^*
$H1$	6.83	6.81	6.81	7.13	7.16	7.74	7.82
$H2$	6.87	6.87	6.87	7.11	7.14	7.72	7.78

TABLE XII. Binding-energy results for the $HB1^*$ model. The last two columns show the accumulative effects of adding consecutively the extra Δ-spectator channels and the $N\Delta$ channels with $2<L\leq 4$, respectively, to the Hannover truncation scheme (see text). The Paris and dispersive (DISP) contributions are given for completeness. The number of channels is indicated in parentheses.

Channels	Paris	DISP	$HB1^*$	ΔSPEC	$2<L(N\Delta)\leq 4$
$J\leq 4$, $\pi=\pm$	7.46 (34)	6.90 (34)	7.96 (53)	7.89 (85)	7.83 (103)
$J\leq 2$, $\pi=\pm$	7.38 (18)	6.83 (18)	7.82 (33)	7.75 (49)	7.69 (57)
$J\leq 2$, $\pi=+$	7.41 (9)	6.93 (9)	7.01 (15)	7.02 (19)	7.03 (21)
$J\leq 1$, $\pi=\pm$	7.10 (10)	6.64 (10)	7.16 (17)	7.06 (21)	7.02 (23)
$J\leq 1$, $\pi=+$	7.30 (5)	6.85 (5)	6.81 (7)		

value, $E_T=7.82$ MeV. The top two rows of Table XII indicate why the 33-ch $HB1^*$ result is in such good accord with the full 103-ch result. Starting with the second row of Table XII, the $J\leq 2$ corrections to the $HB1^*$ 33-ch binding energy yield a loss of about 130 keV of binding, of which about half comes from the additional Δ-spectator channels and half from the inclusion of $L(N\Delta)\geq 3$ channels. Comparison of the dispersive results which include the $L(N\Delta)=3,4$ channels with the corresponding DISP results in Table XII indicates that most of the $L(N\Delta)\geq 3$ contribution actually comes from the associated dispersive effect. Turning to the $J=3,4$ corrections, the $J\leq 4$ $HB1^*$ 53-ch generalization of the Hannover truncation scheme adds about 140 keV to the $HB1^*$ 33-ch binding; relative to the 80-keV increase in the Paris nucleons-only binding (7.46 MeV) this corresponds to an additional one-Δ contribution of about 60 keV. In fact, a 49-ch calculation (not shown) in which just the $J=3,4$ nucleons-only channels are added to the standard $HB1^*$ 33-ch calculation yields $E_T=7.91$ MeV, which differs from the 53-ch result, $E_T=7.96$ MeV, by a 50-keV effect attributable to the additional one-Δ channels in the 53-ch calculation. The $J=3,4$ nucleons-only channels' contribution of 90 keV in this 49-ch calculation differs from that of the purely Paris calculation by only about 10 keV. Because the additional Δ-spectator and $2<L(N\Delta)\leq 4$ channels with $J=3,4$ make essentially no contribution [the Δ-spectator and $L(N\Delta)\geq 3$ corrections for $J\leq 4$ are virtually identical to those of $J\leq 2$], the 140-keV increase in binding represents the net effect of the $J=3,4$ channels. The near cancellation of the 140-keV $J=3,4$ enhancement against the 130-keV loss in binding from the $J\leq 2$ corrections is responsible for the near equality of the 103-ch and 33-ch $HB1^*$ results for E_T.

However, in terms of a net one-Δ effect, the 33-ch $HB1^*$ result implies a net increase in binding of 440 keV, which exceeds the 103-ch figure by about 70 keV. This difference is due to the fact that, while the binding energies of the two cases are nearly identical, in the 103-ch case the nucleons-only contribution is about 80 keV larger. Thus, in comparison, the 103-ch $HB1^*$ result corresponds to a net one-Δ effect of 370 keV, a dispersive effect of 600 keV, and a total three-body-force effect of 970 keV, while the corresponding numbers for the 33-ch $HB1^*$ result are 440, 550, and 990 keV, respectively. These 33-ch figures are close to the original Hannover 33-ch results which are, from Table IX, 390, 580, and 970 keV, respectively. Coincidentally, and partly due to the discrepancy between our 33-ch $HB1^*$ results and those of Ref. [25], the original Hannover 33-ch results are also quite close to our full 103-ch $HB1^*$ results. The complicated set of cancellations just sketched, which is responsible for the near equality of our $HB1^*$ 33-ch and $HB1^*$ 103-ch results for the net one-Δ effect, the appropriate dispersive effect, and the total three-body-force effect, also underlies this coincidence.

Also evident from Table XII is that the dispersive two-body effect grows only slowly from its 5-ch ($J\leq 1$, $\pi=+$) value of 450 keV to its full 34-ch ($J\leq 4$, $\pi=\pm$) value of 560 keV. The 450-keV effect is entirely due to coupling to the ${}^5D_0(N\Delta)$ channel, so that this channel contributes the bulk of the dispersive effect. From Table XII, the next largest contribution to the dispersive effect is the 60 keV from the ($J=2$, $\pi=-$) channels. The $J\leq 4$ result is, in fact, virtually the same as the $J\leq 2$ result, and this remains true when the $L(N\Delta)=3,4$ channels are included. From this it is clear that the one-Δ dispersive effect is already well represented for $J\leq 2$. The fact that the $J=3,4$ dispersive and net contributions of the $L(N\Delta)=3,4$ channels are both negligible implies that the insignificance of these channels is not just due to a cancellation of dispersive and three-body-force contributions. Thus, it is clear that the $L(N\Delta)=3,4$ and Δ-spectator channels with $J=3,4$ are entirely negligible so that the $L(N\Delta)=3,4$ and Δ-spectator channels are also well represented by $J\leq 2$. Table XII then shows that the main contribution of the $L(N\Delta)=3,4$ channels originates with the odd-parity sector (see also Table VI in this respect). In fact, the net contribution of the $L(N\Delta)=3,4$ and Δ-spectator channels is already largely in place for $J\leq 1$. Finally, the full contribution of the $J=3,4$ nucleons-only channels is given (to within about 10 keV) by the difference between the Paris $J\leq 4$ and $J\leq 2$ results, i.e., about 80 keV, while the $J=3,4$ correction due to $L(N\Delta)\leq 2$ is about 50 keV. The net $J=3,4$ correction of 130–140 keV can thus be included to good approximation by simply adding this correction (by hand) to $J\leq 2$ calculations. This is made evident by the top two rows of Table XII and the special 49-ch ($E_T=7.91$ MeV) calculation mentioned earlier, which together show that the $J=3,4$ contribution is insensitive to variations in the $J\leq 2$ channels included.

The next paper in this series presents a nonperturbative

investigation of the effects of ΔΔ degrees of freedom in the trinuclei, again using the Hannover force model (but now with ΔΔ's included). In the ΔΔ case, the number of two- and three-body channels proliferates too rapidly to allow complete calculations beyond $J=1$. It is therefore necessary to start from "core" one-Δ results and investigate ΔΔ effects using an aufbau method which adds and examines the contributions of and correlations between subsets of channels, discarding those which are inessential. The foregoing one-Δ results provide a sound basis upon which to build such ΔΔ investigations. Clearly the neglect of $J=3,4$ channels is likely to be a good approximation, especially given the leading correction to it described above. The neglect of $J\leq 2$ channels with $L(N\Delta)\geq 3$ at least in the initial stages of the ΔΔ investigations also seems warranted and, to a lesser extent, the neglect of Δ-spectator channels with $J=2$ also appears useful. This forms the basis for a realistic investigation of ΔΔ effects in the trinuclei.

V. SUMMARY

The main result of this paper is the 103-ch result for the triton binding energy using the Hannover one-Δ ($H1$) force model: $E_T=7.83$ MeV. This result includes all two- and three-body channels with $J\leq 4$, subject only to the restrictions that the channels contain at most one Δ and have $L(N\Delta)\leq 4$. Compared to the purely Paris nucleons-only figure, $E_T=7.46$ MeV, this corresponds to a net one-Δ contribution to the binding energy of about 370 keV. The $J\leq 4$ one-Δ dispersive effect is found to be 600 keV, implying a full one-Δ three-body-force effect of 970 keV.

This 370-keV result is dissected into contributions from channels of various types. The contribution from channels with $J=3,4$, which have either a Δ spectator or $L(N\Delta)\geq 3$, is found to be negligible. The remaining $J=3,4$ channels contribute about 140 keV, of which about 90 keV derives from inclusion of the nucleons-only channels and about 50 keV from the $L(N\Delta)\leq 2$ channels. This 140-keV figure is found to be insensitive to variations in the $J\leq 2$ channels included in the three-body calculations, so that it can be simply added by hand as a correction to $J\leq 2$ calculations. Similarly, the $J\leq 2$ channels with either $L(N\Delta)\geq 3$ or a Δ spectator coupled to an NN state other than $^1S_0$ are found to reduce the binding by about 130 keV, about half of which comes from the $L(N\Delta)\geq 3$ channels and half from the Δ-spectator channels. The near cancellation of the 140- and −130-keV corrections implies the essential, though basically accidental, correctness of $J\leq 2$ binding-energy calculations which allow only those one-Δ channels with $L(N\Delta)\leq 2$ or with a Δ spectator coupled to the $^1S_0(NN)$ state. Thus, our calculations, which largely confirm the 33-ch results of the original Hannover one-Δ calculations, also validate (albeit only in this specific case) the 33-ch truncation scheme used to obtain them. Our results resolve any uncertainty concerning one-Δ contributions to the triton binding in the Hannover force model. However, the $^1S_0$ effective range of the Hannover one-Δ model is found to be about 0.1 fm too low and this defect could be responsible for about half of the observed 370-keV increase in the triton binding. Finally, several ancillary issues are also addressed in Sec. IV.

The result $E_T=7.83$ MeV is reasonably close to reproducing the actual value $E_T=8.48$ MeV. Because the Paris potential is fitted to proton-proton $^1S_0$ scattering parameters, a charge-dependent correction of about 0.3 MeV must be added to the value $E_T=7.83$ MeV, yielding $E_T\approx 8.13$ MeV, which is not too far removed from the actual value. Unfortunately, ΔΔ effects investigated perturbatively in the original Hannover work reduce the binding by more than 1 MeV and spoil this picture.

Thus, the sequel to this paper investigates trinuclear ΔΔ effects nonperturbatively. With the inclusion of ΔΔ channels, the number of two- and three-body channels proliferates too rapidly to permit complete calculations beyond $J=1$. Thus, ΔΔ effects must be sorted out using a variety of incomplete calculations to determine the important channels. The results of the present paper provide a sound basis on which to build such an analysis. Clearly, the neglect of $J=3,4$ channels is called for and can be partly compensated for by hand. The neglect of $J\leq 2$ channels with $L(N\Delta)\geq 3$ also seems warranted, at least initially, and to a lesser extent the neglect of Δ-spectator channels with $J=2$ also appears useful. This reduces the number of three-body channels with fewer than two Δ's and provides a manageable point of departure for a nonperturbative study of ΔΔ effects in the trinuclei.

ACKNOWLEDGMENT

One of the authors (R.A.R.) would like to acknowledge the support of the Purdue Research Foundation (David Ross Grant No. 6901677).

APPENDIX A: GEOMETRICAL COEFFICIENT

The matrix element

$$\langle pq\alpha|(P_a+P_c)|p'q'\alpha'\rangle \tag{A1}$$

is needed in the derivation of the Faddeev integral equations. While this work is primarily done using J-j coupling, the calculation of this matrix element is more easily done in the $\mathcal{L}$-$\mathcal{S}$ coupling scheme, using the basis vectors

$$|pq\beta\rangle=|pq;(\{(Ll)\mathcal{L},[Ss(n_z)]\mathcal{S}\}\mathcal{J}\mathcal{J}_z;[Tt(n_z)]\mathcal{T}\mathcal{T}_z;NN_z,\tfrac{1}{2}n_z)\rangle\ . \tag{A2}$$

The transformation from one scheme to the other is simply that for recoupling four angular momentum vectors [29], which, in terms of the 9-j symbol, is

$$|pq\alpha\rangle = \hat{J}\hat{j}\sum_{\mathcal{L}\mathcal{S}} \hat{\mathcal{L}}\hat{\mathcal{S}} \begin{Bmatrix} L & l & \mathcal{L} \\ S & s(n_z) & \mathcal{S} \\ J & j & \mathcal{J} \end{Bmatrix} |pq\beta\rangle \ , \tag{A3}$$

where $\hat{x} \equiv \sqrt{2x+1}$. Since the basis states are restricted such that

$$E_1|pq\beta\rangle = -|pq\beta\rangle \ , \tag{A4}$$

$$\langle pq\beta|P_a|p'q'\beta'\rangle = \langle pq\beta|P_c|p'q'\beta'\rangle \ , \tag{A5}$$

it is only necessary to calculate the matrix element of one of the permutation operators.

The method used to calculate the geometrical coefficient in this work is an extension of that of Glöckle [35]. The final form for the matrix element is

$$\langle pq\beta|(P_a+P_c)|p'q'\beta'\rangle = \delta_{\mathcal{J},\mathcal{J}'}\delta_{\mathcal{J}_z,\mathcal{J}'_z}\delta_{\mathcal{T},\mathcal{T}'}\delta_{\mathcal{T}_z,\mathcal{T}'_z}\delta_{\mathcal{L},\mathcal{L}'}\delta_{\mathcal{S},\mathcal{S}'}\delta_{(N_z+n_z),(N'_z+n'_z)} \times \int_{-1}^{+1} dx \frac{\delta(p-p_1(q,q',x))}{p^2} \frac{\delta(p'-p_2(q,q',x))}{p'^2} G_{\beta,\beta'}(q,q',x) \ , \tag{A6}$$

where

$$p_1(q,q',x) = \left| \frac{m(n'_z)}{M(N_z)}\mathbf{q} + \mathbf{q}' \right| \ , \tag{A7}$$

$$p_2(q,q',x) = \left| \mathbf{q} + \frac{m(n_z)}{M(N'_z)}\mathbf{q}' \right| \ , \tag{A8}$$

$$x = \frac{\mathbf{q}\cdot\mathbf{q}'}{qq'} \ , \tag{A9}$$

and

$$G_{\beta,\beta'}(q,q',x) = -\sum_{\bar{n}_z} \langle \tfrac{1}{2}\tfrac{1}{2} n_z \bar{n}_z | N'N'_z\rangle \langle \tfrac{1}{2}\tfrac{1}{2} n'_z \bar{n}_z | NN_z\rangle G_{\mathcal{S}}(\beta,\beta') G_{\mathcal{T}}(\beta,\beta') G_{\mathcal{L}}(\beta,\beta';q,q',x) \ . \tag{A10}$$

The Kronecker δ's in Eq. (A6) just reflect the fact that permutations can change neither the values of the total quantum numbers nor the numbers of nucleons and Δ's present. Unless the quantum number $\bar{n}_z$ simultaneously satisfies

$$\begin{aligned} \bar{n}_z &= N_z - n'_z \\ &= N'_z - n_z \ , \end{aligned} \tag{A11}$$

both of the Clebsch-Gordan coefficients in Eq. (A10) vanish. The spin piece of the geometrical coefficient has the structure

$$G_{\mathcal{S}}(\beta,\beta') = \hat{S}\hat{S}' \begin{Bmatrix} s(n_z) & s(\bar{n}_z) & S' \\ s(n'_z) & \mathcal{S} & S \end{Bmatrix} , \tag{A12}$$

and there is a strictly analogous equation for the isospin piece. The triton is assumed to have $\mathcal{T}=\frac{1}{2}$. The orbital piece is given by

$$G_{\mathcal{L}}(\beta,\beta';q,q',x) = \frac{\hat{L}^2\hat{L}'^2\hat{l}\hat{l}'}{p_1^L p_2^{L'}} \sum_{\substack{0\le\ell\le L \\ n=L-\ell}} \sum_{\substack{0\le\ell'\le L' \\ n'=L'-\ell'}} q'^{\ell'+n} q^{\ell+n'} \begin{bmatrix} 2L \\ 2\ell \end{bmatrix}^{1/2} \begin{bmatrix} 2L' \\ 2\ell' \end{bmatrix}^{1/2} \left[\frac{m(n_z)}{M(N'_z)} \right]^{\ell'} \left[\frac{m(n'_z)}{M(N_z)} \right]^{\ell} \times \sum_k (\hat{k})^2 P_k(x) \sum_{\lambda,\lambda'} (\hat{\lambda}\hat{\lambda}')^2 \begin{bmatrix} \ell' & l' & \lambda' \\ 0 & 0 & 0 \end{bmatrix} \begin{bmatrix} \ell & l & \lambda \\ 0 & 0 & 0 \end{bmatrix} \begin{bmatrix} n' & k & \lambda \\ 0 & 0 & 0 \end{bmatrix} \begin{bmatrix} n & k & \lambda' \\ 0 & 0 & 0 \end{bmatrix} \times \begin{Bmatrix} n' & \ell' & L' \\ l' & \mathcal{L} & \lambda' \end{Bmatrix} \begin{Bmatrix} n & \ell & L \\ l & \mathcal{L} & \lambda \end{Bmatrix} \begin{Bmatrix} n & k & \lambda' \\ n' & \mathcal{L} & \lambda \end{Bmatrix} . \tag{A13}$$

In Eqs. (A12) and (A13), the symbols in curly brackets are 6-j symbols, while the symbols with three columns enclosed by parentheses are 3-j symbols [29]. The function $P_k(x)$ is the usual Legendre polynomial, and the symbols with a single column enclosed by parentheses are binomial coefficients.

The geometrical coefficient which appears in Eq. (25) is then given by

$$G_{\alpha,\alpha'}(q,q',x)=\hat{J}\hat{j}\hat{J}'\hat{j}'\sum_{\mathcal{L}\mathcal{S}}\hat{\mathcal{L}}^2\hat{\mathcal{S}}^2\begin{Bmatrix} L & l & \mathcal{L} \\ S & s(n_z) & \mathcal{S} \\ J & j & \mathcal{J} \end{Bmatrix}\begin{Bmatrix} L' & l' & \mathcal{L} \\ S' & s(n_z') & \mathcal{S} \\ J' & j' & \mathcal{J} \end{Bmatrix}G_{\beta,\beta'}(q,q',x)\ . \tag{A14}$$

When written out fully using the equations above, the geometrical coefficient $G_{\alpha,\alpha'}(q,q',x)$ is fully symmetric under the interchange of primed and unprimed quantities.

APPENDIX B: TWO-BODY t MATRICES

The operator $t(E)$ which satisfies Eq. (21), although similar in form to a two-body t matrix, is actually a three-body operator due to the presence of the three-body Green's-function operator, $G_0(E)$, of Eq. (20). The matrix elements of the potential in the three-body basis of Eq. (13) can be written as

$$\langle pq\alpha|V|p'q'\alpha'\rangle=\delta_{j,j'}\delta_{l,l'}\delta_{n_z,n_z'}\delta_{J,J'}\delta_{T,T'}\delta_{\mathcal{J},\mathcal{J}'}\delta_{\mathcal{J}_z,\mathcal{J}_z'}\delta_{\mathcal{T},\mathcal{T}'}\delta_{\mathcal{T}_z,\mathcal{T}_z'}\frac{\delta(q-q')}{q^2}V^{JT}_{\gamma,\gamma'}(p,p')\ , \tag{B1}$$

where γ is defined in Eq. (27). The first three Kronecker δ's in Eq. (B1) simply reflect the fact that the two-body interaction cannot change the spectator quantum numbers; it is also assumed that the potential is charge independent. Defining, similarly, the function

$$t^{JT}_{\gamma,\gamma'}(p,p';E,q^2,n_z)\ , \tag{B2}$$

Eq. (21) can be reduced to

$$t^{JT}_{\gamma,\gamma'}(p,p';E,q^2,n_z)=V^{JT}_{\gamma,\gamma'}(p,p')+\sum_{\gamma''}\int_0^\infty dp''p''^2V^{JT}_{\gamma,\gamma''}(p,p'')\frac{t^{JT}_{\gamma'',\gamma'}(p'',p';E,q^2,n_z)}{E_2-M(N_z'')c^2-[\hbar^2q^2/2M(N_z'')]-[\hbar^2p''^2/2\mu(N_z'')]}\ . \tag{B3}$$

This is simply the two-body t matrix evaluated at the shifted energy

$$E_2=E-m(n_z)c^2-\frac{\hbar^2q^2}{2m(n_z)}\ , \tag{B4}$$

where the energy E is defined in Eq. (23). The energy E_2 is just the energy available to the pair as measured in the three-body center-of-mass reference frame and the solution of Eq. (B3) is the two-body t matrix in that frame. Unlike its analog in the nucleons-only case, however, this t matrix is not equivalent to the t matrix in the pair rest frame evaluated at the shifted energy $E_2-K_{\text{c.m.}}$, where $K_{\text{c.m.}}$ is the energy associated with the motion of the pair center of mass. The $\hbar^2q^2/2M(N_z'')$ term in Eq. (B3) precludes this connection due to the variability of $M(N_z'')$. The root reason for this is the breaking of Galilean invariance due to the nonconservation of mass in a nonrelativistic framework. Equations (B3) and (B4) deal exactly with the $N\Delta$ mass difference within the context of the model and they represent the closest connection to the t matrix in the pair rest frame.

The practical significance of non-Galilean effects can be gauged by comparing model-exact results based on Eq. (B3) to Galilean invariant results based on a modified version of Eq. (B3) in which $M(N_z'')$ in the term $\hbar^2q^2/2M(N_z'')$ is replaced by $2M_N$, independent of N_z''. Specifically, for the 18-channel $H2$ dispersive case and the 33-channel $HB1^*$ case non-Galilean effects increase the triton binding by about 14 and 18 keV, respectively.

APPENDIX C: NUMERICAL CHECKS

Any extensive computational undertaking such as the one reported in this paper is fraught with the possibility for logical or numerical error. Such errors are not unknown in the previous history of the three-body problem and must be especially carefully guarded against in the present series because its scope represents so substantial an extension beyond well-established computational ground. Thus, this work would be remiss if it did not provide the reader with some indication of the means used to ensure its reliability. Since it is impractical to provide complete details, this appendix summarizes the checking and error-avoidance methods used to ensure the correctness of our results.

The first level of checking involves the basic design of the computational scheme and the direct checks made by the authors. The computational stream of the calculations uses two computer codes for the two-body problem and two codes for the three-body problem. The two-body codes are a potential code which produces the partial-wave-decomposed momentum-space potential and a t-matrix code which produces the corresponding two-body amplitudes at the parametric energies required for the triton calculation. The three-body codes are setup codes which tabulate needed geometrical factors, etc., and the Faddeev code itself. Every part of the coding was checked and cross checked for logic and implementation at least twice by at least two of the authors.

There is one feature of the basic design which is important because it severely restricts the possibilities for error in the programs, both in their logic and in their usage.

Much of the coding implements coupled-channel calculations which need not depend explicitly on the specific nature of individual channels. Thus, it was largely possible to design the codes so that they treat the channels generically, without the need for special branching depending on the Δ content of the channels (the main counterexample being the construction of the Hannover potential, with its *a priori* distinction between NN and $N\Delta$ channels). Since channels containing different numbers of Δ's are treated largely in the same way, with the introduction and use of the "n-spin" quantum number it is only necessary to specify and keep track of the quantum numbers of the two-body amplitudes and the three-body channels. This information is stored in two character arrays which link together and completely control all four of the main computer codes. The four codes accept and process these arrays independently of the Δ content of individual channels. Specification of these two arrays is all that is required to define and vary the physical circumstance of interest. Thus, most of the computational machinery is actually "blind" to the distinction between nucleons and Δ's, and is fully validated by checks of the nucleons-only problem.

At the second level, many numerical evaluations of representative values of quantities or of limiting cases were used to check specific sections of the computer codes. Virtually every part of the coding which could not be checked either by such devices or by direct comparison with well-known results was validated by performing tasks in two independent ways. Often this involved replacing sets of subroutines with those relevant to the alternative approach. The most extensive example of such checking by duplication was our construction of the Hannover-model partial-wave potentials using independent r-space and k-space approaches.

On the third level were comprehensive checks of the entire computational system utilizing known results from the two- and three-body problems. In the nucleons-only case, the full stream was checked by verifying consistency with known two- and three-body results for the Paris and Bonn potentials. Given this check, it was then possible to fully check the dispersive $N\Delta$ case. Having checked the construction of the potential by duplication and the nucleons-only three-body calculation using known Paris and Bonn results, all that was required was to check the implementation of the Hannover renormalization scheme and the handling of $N\Delta$ channels by the t-matrix code. These were checked in two ways. First, as noted in the text, the Hannover potential model is designed so that the NN-sector t matrices precisely reproduce the Paris t matrices at the renormalization energy E_r. This property was confirmed for our calculations (for several different values of E_r), implying consistency between the t-matrix code and the implementation of the Hannover-model renormalization scheme by the potential code. Second, in the $N\Delta$ dispersive case, the same triton binding, and, in fact, the same NN-sector t matrices, must result from the direct calculation and from an alternative calculation which uses no explicit NN-$N\Delta$ coupling but uses, in the NN sector, the effective potential of Eq. (36). This was verified for our calculations, validating the handling of $N\Delta$ channels by the t-matrix code (note that the direct calculation involves $N\Delta$ channels in the t-matrix code, whereas the calculation using $V_{\rm eff}$ does not).

TABLE XIII. Numerical stability of the binding energy for the $HA2$ model. The first two columns show the number of quadrature points and the cutoff for the q' integration, respectively. The third column contains the number of quadrature points for the x' integration, and the last column shows the binding-energy result.

N_q	C_q (fm^{-1})	N_x	E_T (MeV)
10	2.8	10	6.762
10	3.0	10	6.792
10	3.2	10	6.818
12	3.2	10	6.821
12	3.4	10	6.842
12	3.6	10	6.858
12	4.0	10	6.874
12	4.0	12	6.874
14	5.5	10	6.874
16	5.5	10	6.874
24	6.0	10	6.876

This concludes the summary of our checking methods. Although the three-body codes are largely blind to the Δ content of the channels, and are therefore largely checked by the nucleons-only checks, it would be preferable to have a definitive test using a previous result. The one-Δ results reported in the text are very close to the results of Ref. [25], and the differences are probably irrelevant from a physical point of view. However, the differences are numerically significant and are not at the level of computational noise. The fact that our results differ most from those of Ref. [25] for the dispersive case unfortunately precludes a clear check of the handling of one-Δ channels by our three-body codes.

Finally, the numerical discretizations used to approximate the continuous variables present in the calculations (p, q', and x') were tested for stability. The discretization of the variable p is important only in the solution of the two-body Lippmann-Schwinger equation, and presents no difficulties. The solution of Eq. (25) uses the standard iteration technique first applied to this problem by Malfliet and Tjon [36,37]. The infinite integral over the spectator momentum q' is approximated by a finite integral from zero to a cutoff momentum C_q. This and the x' integral are then approximated by a Gauss-Legendre quadrature. The numerical accuracy of these approximations was tested by solving Eq. (25) for increasing values of the cutoff momentum and the number of quadrature points. The stability of the binding energy to the numerical approximations is summarized in Table XIII for the specific case of the Hannover $H2$ dispersive calculation. The values $N_q=14$, $C_q=5.5$ fm^{-1}, and $N_x=10$ have been taken as the standard choices throughout this work. The quoted binding-energy results, aside from Table XIII, have been rounded off to the nearest 10 keV, and it is felt that these results are numerically stable to within ± 10 keV.

[1] See, for example, *Mesons in Nuclei,* edited by M. Rho and D. Wilkinson (North-Holland, Amsterdam, 1979), Vols. I–III.
[2] L. D. Faddeev, Zh. Eksp. Teor. Fiz. **39**, 1459 (1961) [Sov. Phys. JETP **12**, 1014 (1961)].
[3] L. D. Faddeev, *Mathematical Problems of the Quantum Theory of Scattering for a Three-Particle System* (Davey, Daniel and Co., Hartford, 1965).
[4] For a review of the three-body problem, see, for example, J. L. Friar, B. F. Gibson, and G. L. Payne, Comments Nucl. Part. Phys. **11**, 51 (1983).
[5] R. V. Reid, Ann. Phys. (N.Y.) **50**, 411 (1968).
[6] M. Lacombe, B. Loiseau, J. M. Richard, R. Vinh Mau, J. Côté, P. Pirès, and R. de Tourreil, Phys. Rev. C **21**, 861 (1980).
[7] R. B. Wiringa, R. A. Smith, and T. L. Ainsworth, Phys. Rev. C **29**, 1207 (1984).
[8] K. Holinde and R. Machleidt, Nucl. Phys. **A247**, 495 (1975).
[9] R. Machleidt, Adv. Nucl. Phys. **19**, 189 (1989).
[10] R. Machleidt, K. Holinde, and Ch. Elster, Phys. Rep. **149**, 1 (1987).
[11] R. A. Brandenburg, G. S. Chulick, R. Machleidt, A. Picklesimer, and R. M. Thaler, Phys. Rev. C **37**, 1245 (1988).
[12] R. A. Brandenburg, G. S. Chulick, R. Machleidt, A. Picklesimer, and R. M. Thaler, Phys. Rev. C **38**, 1397 (1988).
[13] J. Fujita and H. Miyazawa, Prog. Theor. Phys. **17**, 360 (1957).
[14] S. A. Coon, M. D. Scadron, P. C. Mcnamee, B. R. Barrett, D. W. E. Blatt, and B. H. J. McKellar, Nucl. Phys. **A317**, 242 (1979).
[15] H. T. Coelho, T. K. Das, and M. R. Robilotta, Phys. Rev. C **28**, 1812 (1983).
[16] C. R. Chen, G. L. Payne, J. L. Friar, and B. F. Gibson, Phys. Rev. Lett. **55**, 374 (1985).
[17] C. R. Chen, G. L. Payne, J. L. Friar, and B. F. Gibson, Phys. Rev. C **33**, 1740 (1984).
[18] S. Ishikawa and T. Sasakawa, Phys. Rev. Lett. **56**, 317 (1986).
[19] S. Ishikawa and T. Sasakawa, Few-Body Syst. **1**, 3 (1986).
[20] S. Ishikawa and T. Sasakawa, Few-Body Syst. **1**, 143 (1986).
[21] A. Bömelberg, Phys. Rev. C **34**, 14 (1986).
[22] K. Holinde and R. Machleidt, Nucl. Phys. **A280**, 429 (1977).
[23] R. A. Smith and V. R. Pandharipande, Nucl. Phys. **A256**, 327 (1976).
[24] G.-H. Niephaus, M. Gari, and B. Sommer, Phys. Rev. C **20**, 1096 (1979).
[25] Ch. Hajduk, P. U. Sauer, and W. Strueve, Nucl. Phys. **A405**, 581 (1983).
[26] Ch. Hajduk, P. U. Sauer, and S. N. Yang, Nucl. Phys. **A405**, 605 (1983).
[27] M. T. Peña, H. Henning, and P. U. Sauer, Phys. Rev. C **42**, 855 (1990).
[28] The original Hannover calculations used the force model referred to in this work as the "Hannover* model" and current Hannover calculations also use this model, M. T. Peña and P. U. Sauer, private communication; Ch. Hajduk, private communication.
[29] D. M. Brink and G. R. Satchler, *Angular Momentum,* 2nd ed. (Clarendon, Oxford, 1968).
[30] A. R. Edmonds, *Angular Momentum in Quantum Mechanics* (Princeton University, Princeton, 1957).
[31] A. de-Shalit and I. Talmi, *Nuclear Shell Theory* (Academic, New York, 1963).
[32] J. Haidenbauer and W. Plessas, Phys. Rev. C **30**, 1822 (1984).
[33] V. F. Kharchenko, N. M. Petrov, and S. A. Storozhenko, Nucl. Phys. **A106**, 464 (1968).
[34] B. F. Gibson and G. J. Stephenson, Jr., Phys. Rev. C **8**, 1222 (1973).
[35] W. Glöckle, Nucl. Phys. **A381**, 343 (1982).
[36] R. A. Malfliet and J. A. Tjon, Nucl. Phys. **A127**, 161 (1969).
[37] R. A. Malfliet and J. A. Tjon, Phys. Lett. **29B**, 391 (1969).